Zhang *et al. PhotoniX* (2023) 4:24
https://doi.org/10.1186/s43074-023-00101-8

PhotoniX

REVIEW Open Access

# Ultrafast laser-induced self-organized nanostructuring in transparent dielectrics: fundamentals and applications

Bo Zhang[1*], Zhuo Wang[1], Dezhi Tan[2] and Jiangrong Qiu[1*]

*Correspondence: zhangbob@zju.edu.cn; qjr@zju.edu.cn

[1] State Key Laboratory of Modern Optical Instrumentation, College of Optical Science and Engineering, Zhejiang University, Hangzhou, China
[2] Zhejiang Lab, Hangzhou, China

**Abstract**

Inscribing functional micro-nano-structures in transparent dielectrics enables constructing all-inorganic photonic devices with excellent integration, robustness, and durability, but remains a great challenge for conventional fabrication techniques. Recently, ultrafast laser-induced self-organization engineering has emerged as a promising rapid prototyping platform that opens up facile and universal approaches for constructing various advanced nanophotonic elements and attracted tremendous attention all over the world. This paper summarizes the history and important milestones in the development of ultrafast laser-induced self-organized nanostructuring (ULSN) in transparent dielectrics and reviews recent research progresses by introducing newly reported physical phenomena, theoretical mechanisms/models, regulation techniques, and engineering applications, where representative works related to next-generation light manipulation, data storage, optical detecting are discussed in detail. This paper also presents an outlook on the challenges and future trends of ULSN, and important issues merit further exploration.

**Keywords:** Ultrafast laser, Self-organization, Nanostructuring, Transparent dielectrics

## Introduction

As Moore's law going close to its limit, integrated photonics aiming for on-chip functionalization is fast-rising and has brought up a boom in searching for next-generation optoelectronic substrate materials. Especially, all-inorganic transparent dielectrics such as various glasses and crystals have been established as excellent modular platforms for light emission [1–5], transmission [6–9], and modulation [10–15]. Predictably, next-generation integrated photonic elements and systems will largely rely on various three-dimensional (3D) micro-nano structures inscribed in transparent dielectrics [16–22], such as optical waveguides [23–26], optical couplers [27–29], photonic crystals [30–32], and optical storage voxels [33–35], which has arisen an ever-growing demand for the fabrication of highly integrated all-inorganic optical devices and systems. Currently, it remains difficult and a major challenge to build complex 3D micro-nano structures in multiple all-inorganic transparent dielectrics by using conventional lithography fabrication technologies, owing to the extremely low linear optical absorption and high

Springer Open

© The Author(s) 2023. **Open Access** This article is licensed under a Creative Commons Attribution 4.0 International License, which permits use, sharing, adaptation, distribution and reproduction in any medium or format, as long as you give appropriate credit to the original author(s) and the source, provide a link to the Creative Commons licence, and indicate if changes were made. The images or other third party material in this article are included in the article's Creative Commons licence, unless indicated otherwise in a credit line to the material. If material is not included in the article's Creative Commons licence and your intended use is not permitted by statutory regulation or exceeds the permitted use, you will need to obtain permission directly from the copyright holder. To view a copy of this licence, visit http://creativecommons.org/licenses/by/4.0/.

modification threshold of these materials. Therefore, novel approaches for tailoring transparent dielectrics to efficiently construct complicated functional micro-nano structures are urgently needed.

Ultrafast laser is among the greatest scientific breakthroughs in the twentieth century. Benefiting from its extremely high peak power (up to the PW level [36]), an ultrafast laser can easily excite a strong non-linear light absorption, enabling various intriguing strong field material modifications [37–43], which greatly expands human's understanding of light-matter interaction under extreme physical conditions. As a consequence, a large number of new phenomena induced by ultrafast laser have been observed one after another since entering the twenty-first century, giving birth to many advanced processing technologies, such as nanomaterial synthesis [44–48], two-photon polymerization [49–51], laser ablation [52–55], selective crystallization [56–58], ion valence manipulation [59–61], and etching assisted laser modification [62–64], etc. Among them, ultrafast laser-induced self-organized nanostructuring (ULSN) is especially fascinating and has established itself to be a fertile ground for exploring novel optical fabrication methodologies because of its high efficiency, super-resolution, and controllability in creating functional surface nanostructures [65–70]. After nearly 30 years of development, ULSN optics is currently developing into a systematic research topic that covers new phenomenon observation, fundamental theory establishment, regulation technique exploration, and engineering applications. Especially in recent years, boosted by multidisciplinary fields such as big data, artificial intelligence, integrated optics, advanced sensing and detecting, 3D spatial ULSN in transparent dielectrics has become a rising new hotspot and attracted extensive attention.

In this paper, we review the developmental path of ULSN in transparent dielectrics and focus on important phenomena, hypotheses, theories, and applications. The milestone research works in recent ten years made by major research groups all over the world are introduced in detail and the existing issues as well as research gaps are discussed. Finally, the future development trend of ULSN methodology and ULSN-related technologies is prospected.

## Ultrafast laser-induced self-organization phenomena in transparent dielectrics

Although photo-induced periodic self-organization has been extensively discussed on the surfaces of different materials ( including transparent dielectrics) since the laser was invented in 1960 [71], it was not until 2003 that the first report on ULSN in transparent dielectrics appeared [72]. Up to now, a universal physical picture of ULSN in various transparent dielectrics remains far from being achieved, which is attributed to the particularity of ULSN in transparent dielectrics. For ULSN on surfaces, the inherent substrate-air interface and its initial nanoroughness provide suitable conditions for plasma excitation and local field enhancement where the optical field evolution study can be well set on a 2D plane [73–76]. However, no naturally existing interface is available in transparent dielectrics, and physical models for describing ULSN processes are generally needed to be considered in 3D space [77–79]. The observation, manipulation, and characterization of the structures induced in transparent dielectrics are also much more difficult than those on surfaces. For ULSN in transparent dielectrics, more factors will participate in the laser-matter interaction process and usually cannot be ignored [80, 81],

for example, intrinsic structural properties of the matrix (defects and inhomogeneities in lattices or glass networks) [82], light propagation behaviors in the media (refraction, scattering, and self-focusing, etc.) [83], and state changes of materials (metallization, phase transition, and refractive index change, etc.) in 3D space [84, 85], which makes ULSN phenomena in transparent dielectrics widely divergent. Therefore, it is necessary to conduct a targeted review and discussion on the phenomena, mechanisms, and applications of ULSN in different transparent media.

With the substantial development of ultrafast laser processing and material characterization technologies over the last 20 years, a large number of ultrafast laser-induced self-organization phenomena that involve new light-matter interaction mechanisms have been successively uncovered in various transparent dielectrics, serving as the origin of novel ULSN technologies. Representative examples include periodic crystallization, periodic micro-nano voids/pores, and nanogratings in glasses and crystals. These phenomena lead to the birth of multiple ULSN technical routes of near-field enhancement patterning, self-organized lithography, and laser-assisted etching, which is followed by a series of unique ULSN-based applications, such as micro-nano photonic elements, multi-dimensional optical data storage, and micro-nano fluidic devices (Fig. 1).

## Nanogratings

The discovery of nanograting structure can be traced back to the year 1999 when L. Sudrie et al. [86] reported an extraordinary anisotropic light scattering induced

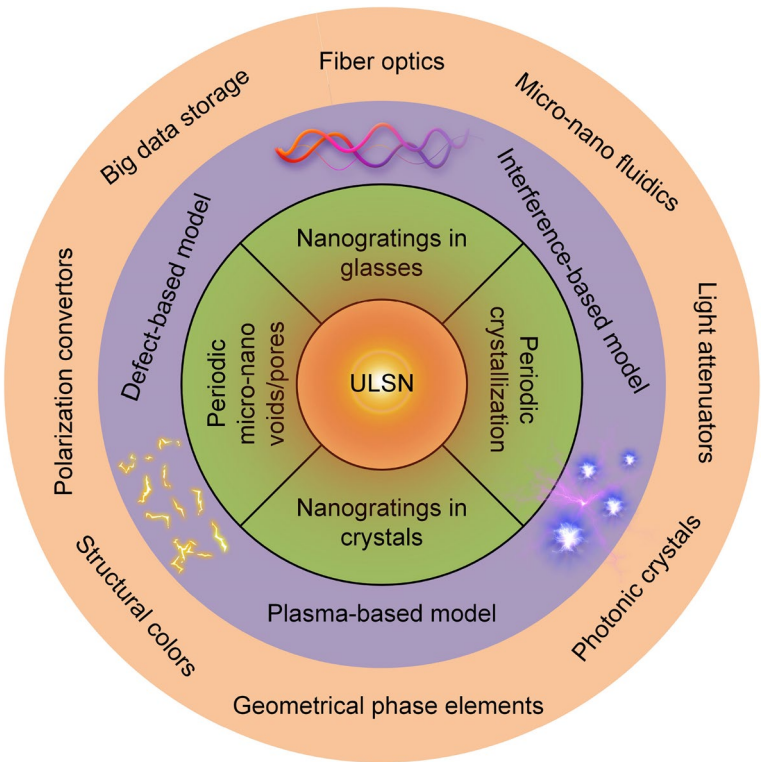


**Fig. 1** Schemes for ULSN-induced phenomena, corresponding mechanisms and applications of the created structures

by femtosecond laser irradiation in fused silica. In the same year, Kazansky et al. [87] observed a similar phenomenon inside germanium-doped silica glass. Qiu et al. [88] then reported a polarization-dependent optical scattering in a fluoroaluminate glass, and attributed this phenomenon to the creation of a permanent nanostructure in the laser-irradiated area. In 2003, Shimotsuma et al. [72] finally revealed an unprecedented polarization-dependent nanometer-sized grating structure in the plane perpendicular to the ultrafast laser propagation direction by using backscattering electron microscopy (Fig. 2(a)). Further characterization indicates that nanograting is formed in a carrot-shaped 3D region along the laser propagation direction (Fig. 2(b)) [89–91], which is considered caused by the self-focusing effect, spherical aberration effect, and other nonlinear effects of ultrafast laser-matter interaction [92–94]. In the following ten years, various physicochemical characteristics of nanograting were revealed one after another, including structural anisotropic periodicity [82, 95], polarization-dependent birefringence (Fig. 2(c)) [96], selective etching (Fig. 2(d)) [91, 97], erasing and rewriting capacity (Fig. 2(e)) [98], and heat resistance (Fig. 2(f)) [99, 100], which lays the foundation of the establishment of ULSN technology and ULSN-based applications.

As a symbolic feature of nanograting, periodicity is essentially reflected by periodic material modulations. The most common example is periodic oxygen modulation [99, 101]. Auger electron spectroscopic analysis of the nanograting formed in fused silica shows that oxygen in the laser-irradiated area is periodically modulated [72]. The oxygen content in the dark regions of the periodic fringes is lower, while silicon remains almost unchanged. Shimotsuma et al. [102] subsequently confirmed that oxygen-deficient zones are periodically arranged nanoplates that are filled with nanopores with a feature size of about 10 nm. These oxygen-deficient nanoplates possess a much lower refractive index (RI) compared with the

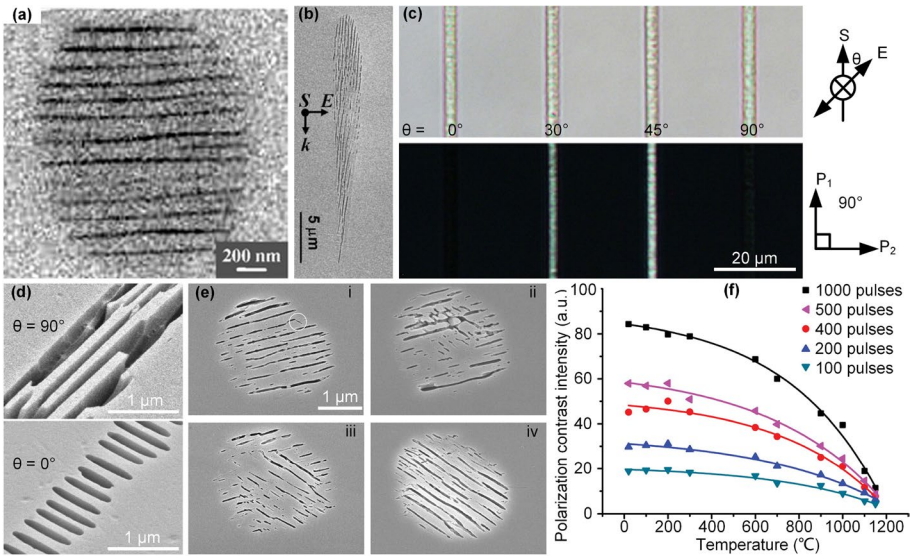


**Fig. 2** **a** Nanogratings induced in fused silica [72]. Copyright 2003, American Physical Society. **b** Cross section view of nanogratings [91]. Copyright 2006, Springer Nature. **c** Polarization-dependent birefringence of nanogratings [96]. Copyright 2014, Optica Publishing Group. **d** Polarization-dependent selective etching of nanogratings [97]. Copyright 2005, Optica Publishing Group. **e** Erasing and rewriting capacity of nanogratings [98]. Copyright 2007, Optica Publishing Group. f Heat resistance of nanogratings [100]. Copyright 2012, Laser Institute of America

surrounding glass matrix (RI change can be as high as 0.2 [103]) and are highly susceptible to hydrofluoric acid (Fig. 2(d)) [97]. These physicochemical anisotropies of nanograting make the originally isotropic glass matrix possess some crystalline properties.

In 2004, Bricchi et al. [104] investigated the birefringence of nanograting and attributed this phenomenon to the optical phase modulation caused by the subwavelength periodic refractive-index distribution. Numerous subsequent studies have confirmed that the appearance of polarization-dependent optical birefringence is a basic criterion for the formation of nanogratings [96, 105]. This artificial birefringence signal can not only be used to optimize the processing parameters of ULSN but also serve as an information carrier, playing an important role in high-density optical storage. In 2008, Taylor et al. [90] presented the erasing and overwriting process of nanogratings in fused silica. There, the rewritten structures emerge immediately within the first three ultrafast laser pulses and gradually grow along the direction perpendicular to the rewrite laser polarization with the increase of incident pulses (Fig. 2(e)). In this process, the origin nanograting is gradually erased and replaced by the rewritten one with a new orientation, which can also be characterized by the birefringence signal of the rewriting area. The rewritable property makes nanograting an ideal tool for ULSN-based optical data storage.

Heat resistance is a key performance of various all-inorganic functional elements. However, many ultrafast laser-produced structures are metastable state structures that are easily changed through thermal excitation, such as color centers and excitons [106, 107]. Therefore, investigating the heat resistance of nanograting is necessary. In 2012, Richter et al. [100] studied the thermal stability of the nanograting induced in fused silica with different incident pulse numbers by detecting the birefringence intensity (Fig. 2(f)). Experiments indicate that heat treatment gradually weakens the birefringence signal of nanograting, indicating that nanograting is deteriorating. Notably, the birefringence signal does not disappear before the melting temperature of fused silica is reached and remains 13% of the initial intensity after being treated with a temperature of 1150 ℃. In 2022, Wang et al. [108] systematically examined the thermal stability of nanogratings induced in silica-based glasses and confirmed that high levels of OH and Cl impurities will reduce the thermal stability, but the overall excellent heat resistance of nanograting still makes nanogratings a promising candidate in building highly robust elements.

As the most fundamental and widely reported structure induced by ULSN in transparent dielectrics, nanogratings possess plenty of representative features that can be universally extended to other ULSN-produced self-organization forms. With the development of characterization techniques and detecting methods, more work is needed to further generalize the theoretical framework of nanogratings, boosting the mechanism and application research on ultrafast laser-matter interaction physics.

#### Periodic crystallization

Since the discovery of nanograting in fused silica, researchers have been working on extending ULSN to more functional transparent dielectrics [109]. Studies have shown that most nanogratings consist of periodic defect phases, while, in some unconventional glasses, similar grating structures can appear in the form of periodic crystallization.

In 2016, Cao et al. [110] first reported an extraordinary periodic crystallization phenomenon in $Li_2O$-$Nb_2O_5$-$SiO_2$ glass and have done systematic works on this structure in the following years [111–113]. Crystallographic characterization indicates that this self-assembled nanostructure consists of periodically arranged nanocrystals embedded in the glass matrix. These nanocrystal polar axes are aligned perpendicular to the laser polarization, which preliminarily indicates that the ultrafast laser-induced periodic crystallization in the unconventional glass is polarization-dependent (Fig. 3(a)-(c)). The research group believes that these layered crystalline nanostructures hold the potential to support tunable second-harmonic generation and serve as nonlinear photonic elements. However, limited by the poor regularity of this nanostructure, they have not demonstrated its practical application.

In 2018, Shimotsuma et al. [114] observed another polarization-dependent periodic crystallization structure in $Al_2O_3$-$Dy_2O_3$ glass (Fig. 3(d)), and found that by adjusting the content of $Dy_2O_3$ in the glass, two types of crystallites can be precipitated. Raman spectroscopy indicates that for Al-30Dy glass ($Dy_2O_3$ content is 30 mol%), the precipitated crystal is $Dy_3Al_5O_{12}$ garnet, while for Al-40Dy glass ($Dy_2O_3$ content is 40 mol%), the precipitated crystal can be $Dy_3Al_5O_{12}$ garnet or $DyAlO_3$ perovskite crystals according to the pulse energy. Structural characterization shows that the periodic crystallization induced in $Al_2O_3$-$Dy_2O_3$ glass possesses fairly high regularity and controllability, which confers its broader application prospects.

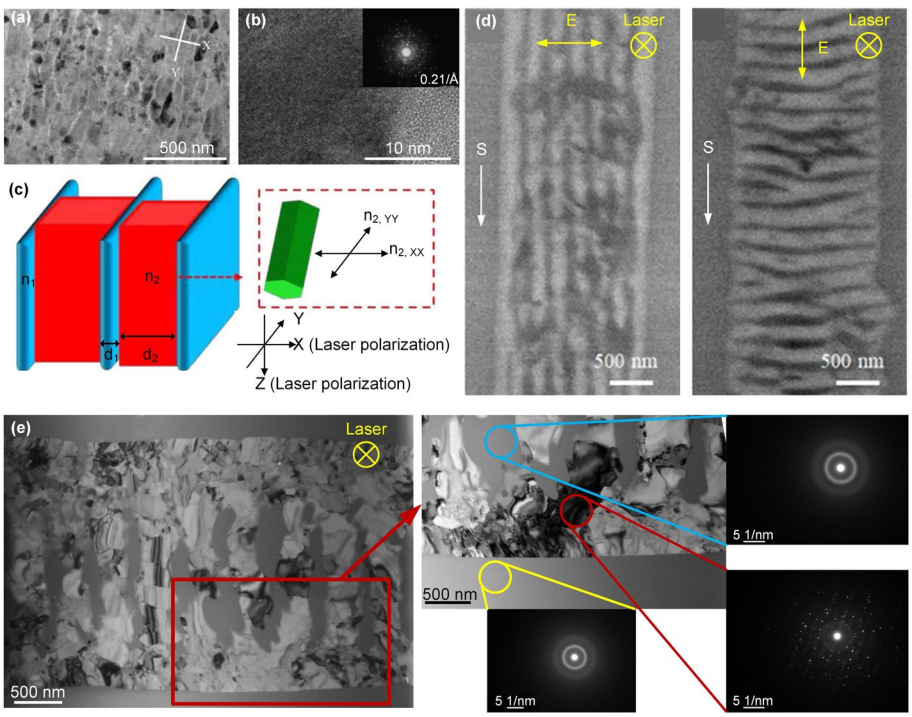


**Fig. 3** **a** Periodic crystallization induced in lithium niobium silicate glass and **b**) corresponding high-resolution transmission electron microscopy (HRTEM) image of the crystal-glass interface. **c** Schematic of ULSN-produced periodic crystallization [110]. Copyright 2016, Optica Publishing Group. **d** Periodic crystallization induced in $Al_2O_3$-$Dy_2O_3$ glass [114]. Copyright 2018, Springer Nature. **e** Periodic crystallization induced in LTN glass and corresponding transmission electron microscopy (TEM) structural characterization [115]. Copyright 2019, Wiley–VCH

In 2019, Zhang et al. [115] reported a periodic crystalline structure in a $La_2O_3$-$Ta_2O_5$-$Nb_2O_5$ (LTN) glass system (Fig. 3(e)), and studied the effects of glass composition and laser parameters on the ultrafast laser-induced periodic crystallization process. Experiments indicate that the birefringence signal of the induced periodic crystalline structure increases significantly with the increase of $Ta_2O_5$ content, while in $La_2O_3$-$Nb_2O_5$ glass without $Ta_2O_5$, it is extremely difficult to induce periodic crystallization. This is because the addition of $Ta_2O_5$ enhances the crystallization ability of the glass system and plays a role in promoting nucleation. Notably, this study also demonstrated the polarization-dependent light attenuation performance of periodic crystalline structures in the near-infrared region, which is the first application demo based on this structure. In 2021, Zhang et al. [116] further demonstrated that the birefringence signal of periodic crystallization structures can be erased and rewritten by an ultrafast laser with a different polarization state, implying a considerable degree of similarity between periodic crystallization and nanogratings.

Ultrafast laser-induced periodic crystallization has just been revealed in recent years and is still in its infancy, but is rapidly developing to become a brand new research field where a large number of research gaps related to physical phenomena, theoretical models, and engineering applications are waiting to be addressed. In the future, by combining various frontier optical technologies like spatial light modulation (SLM), beam shaping, multi-beam interference, and super-resolution processing, ultrafast laser-induced periodic crystallization is expected to serve as a highly efficient and universal method for in situ constructing functional phase transition structures in various mainstream optical media, empowering next-generation integrated optics research.

#### Other self-organization forms

Owing to the complexity of ultrafast laser-matter interaction in transparent dielectrics, the material modifications induced by ultrafast laser vary widely depending on the irradiation conditions and the types of target materials. Since the discovery of nanogratings, more and more ULSN-produced peculiar phenomena and micro-nano structures in transparent materials have been uncovered, such as periodic micro-nano voids, anomalous polarization-dependent structures, and periodic structures in crystals, which greatly expands ULSN-based material modification and deepens people's understanding of strong field light-matter interaction physics.

In 2005, Kanehira et al. [117] first reported a periodically aligned nanovoid structure in conventional borosilicate glass via single femtosecond laser irradiation. The induced nanoscaled spherical voids were self-organized with a period along the laser propagation direction and can be manipulated by tuning laser parameters and focusing position (Fig. 4(a)). Since then, ultrafast laser-induced periodic micro-nano voids have been observed in fused silica [118], $SrTiO_3$ crystal [119], $CaF_2$ crystal [120], $Al_2O_3$ crystal [121], and glasses [122] one after another, revealing the high universality of this process. For structural manipulation, Hu et al. [123] presented that by moving the laser focusing position close to the surface perpendicular to the horizontal surface (XY plane) of the sample, the one-step creation of two perpendicular strings of periodic voids can be achieved. Song et al. [124] reported that by employing different types of objective lens, inverted periodic voids with opposite directions can be

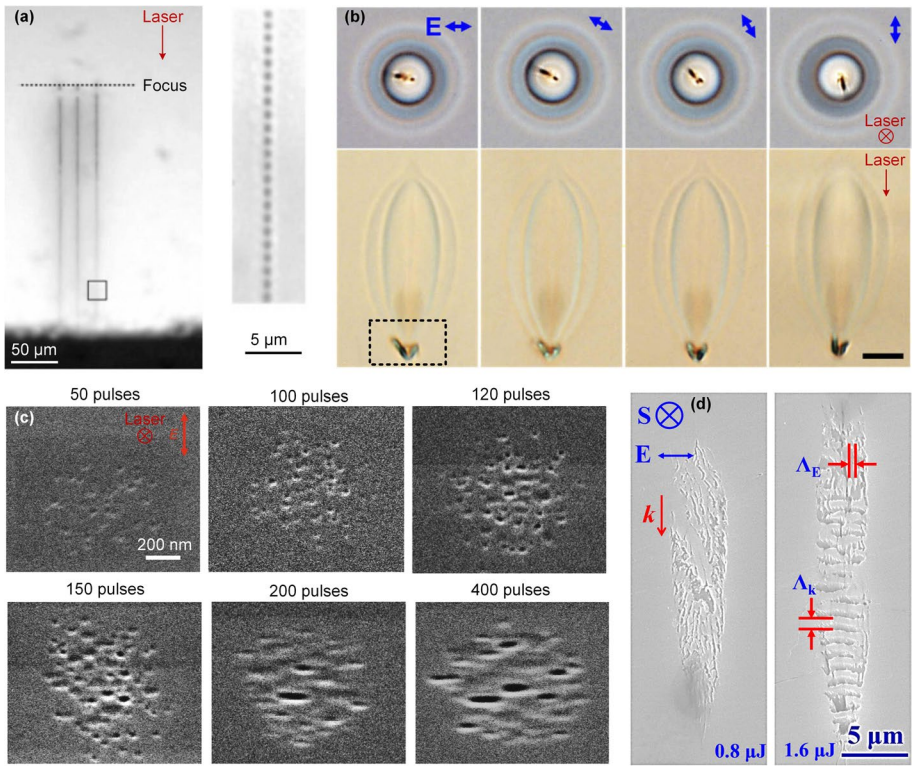


**Fig. 4** **a** Periodically aligned nanovoids induced in borosilicate glass [117]. Copyright 2005, American Chemical Society. **b** Polarization-dependent V-shaped structure (marked by dotted box) induced in aluminosilicate glass [126]. Copyright 2021, Optica Publishing Group. **c** SEM images of the polarization-dependent nanopores written with different pulse numbers [127]. Copyright 2020, Nature Springer. **d** SEM images of cross sections of the multiple periodic structures inscribed in quartz crystal [128]. Copyright 2019, Optica Publishing Group

induced. In 2011, Luo et al. [125] presented that inverted periodic voids can also be achieved by tuning the objective's immersion liquid, showing the flexible controllability of this self-organized structure.

In 2016, Zhang et al. [129] observed an anomalous polarization-dependent dumbbell-shaped structure by using ultrafast laser static irradiation in an aluminosilicate glass. This dumbbell-shaped structure is formed at the top of the laser focal volume and can be erased by further irradiation. Interestingly, $O^2$ bubbles are revealed to appear at the periphery of the incident laser beam and distribute along the laser polarization direction. In 2021, they further reported a V-shaped crack that forms at the bottom of the laser-modified volume and is oriented parallel to the laser polarization (Fig. 4(b)) [126]. These findings enrich the family of non-periodic self-organized structures. Sakakura et al. [127] recently presented brand new polarization-dependent nanopores by ULSN in fused silica that share many optical properties of nanogratings, such as structural anisotropy, birefringence, and polarization-dependence (Fig. 4(c)). The formation of this structure is considered attributed to the interstitial oxygen generation caused by ultrafast laser-induced multiphoton and avalanche ionization. Notably, these nanopores are superior to conventional nanogratings in terms of reducing incident pulse number, pulse energy, and optical loss, which make them

competitive in constructing ultralow-loss optical elements and high-speed optical data storage.

Except for glasses, ULSN has been demonstrated in more types of dielectrics. In 2016, Karpinski et al. [130] induced a self-organized periodic planar structure in MgO-doped $LiNbO_3$ crystal by using ultrafast laser continuous writing. Scanning electron microscopy (SEM) images confirm that such a periodic structure is periodically assembled and aligned perpendicular to the laser polarization, which is highly similar to the nanogratings formed in glasses. In 2019, Zhang et al. [128] reported another unique self-organization phenomenon in bulk quartz crystal (Fig. 4(d)). There, three types of periodic structures with different periods are simultaneously induced in the irradiation volume. The first one is similar to nanogratings and the second one is formed in the laser writing direction. The third one is formed in the laser propagation direction. In 2021, Xu et al. [131] and Zhai et al. [132] inscribed nanograting-like self-organized periodic structures in sapphire that possess optical phase modulation, erasing, and rewriting abilities. Notably, a new class of ULSN mediating between the surface and the interior has also been rising in recent years. In these studies, metal nanoparticles (NPs) or clusters with nonlinear optical responses are introduced into transparent dielectrics to modulate incident light waves and establish a periodic field distribution, thereby activating ULSN [133–135]. The self-assembled periodic structures are usually produced in thin films or near-surface regions owing to the limitation of ion deposition or implantation depth [136]. These results expand ULSN methods to more functional materials like bulk crystals, films, and composite materials, which helps to clarify the linkages of different ULSN phenomena and enriches the potentially available materials.

As important branches of ULSN, the discovery of these novel self-organization phenomena is encouraging, as they greatly generalize ULSN approach in product categories, manipulation degrees of freedom, and available materials. By utilizing the optical modulation abilities of the created structures, various novel tools for constructing photonic elements can be developed in the future. However, the research on these structures is still not thorough and limited to the interpretation of experimental observations, and their formation mechanisms remain largely unclear. As a result, these ULSN methods are currently far from mature whether in theory or technological practice. Therefore, more studies need to be carried out to fully clarify the physical processes behind them, improve the regularity of products, and explore structural manipulation methods.

## Mechanisms of ultrafast laser-induced self-organization in transparent dielectrics

The ultrafast laser-matter interaction is a highly complex multi-physics coupling process involving various nonlinear effects that are currently still far from fully clarified. As a typical instance of ultrafast laser-matter interaction, ULSN in transparent dielectrics remains largely enigmatic. In the last 20 years, researchers have invested tremendous efforts to uncover its physical mechanisms and a series of inspiring hypotheses, models, and concepts have been proposed, which greatly promotes the process of fully understanding and utilizing ULSN. Here, we mainly focus on the representative research progress and important milestones in recent years.

### Interference-based model

The theoretical frameworks for early discovered ULSN phenomena are relatively well established. With the first observation of the nanogratings in fused silica, Shimotsuma et al. [72, 137] preliminarily proposed an interference model similar to the formation mechanism of surface periodic structures [71]. In this model, the nonlinear ionization process in the laser irradiation area releases plenty of free electrons, resulting in the creation of electron plasmas. This process will greatly promote light absorption and then lead to the excitation of plasma waves. The interference between this electron plasma wave and subsequent incident light wave finally induces the creation of nanogratings in transparent media. This model well explains the structural periodicity (Fig. 5(a)) and has been considered the most important origin theory for nanograting phenomena. Since then, a series of studies have been carried out to improve the original interference theory [79, 138, 139]. These works revealed that the periodic field distribution can be established and modulated by various scattering centers originating from inhomogeneities, electronic defects, and laser-induced nanopores/voids in the media (Fig. 5(b)). In a simple view, the interference of the incident waves and the scattered waves from scattering results in the wavelength-scaled periodicity perpendicular to the laser polarization [138], and the coherent superposition of multiple

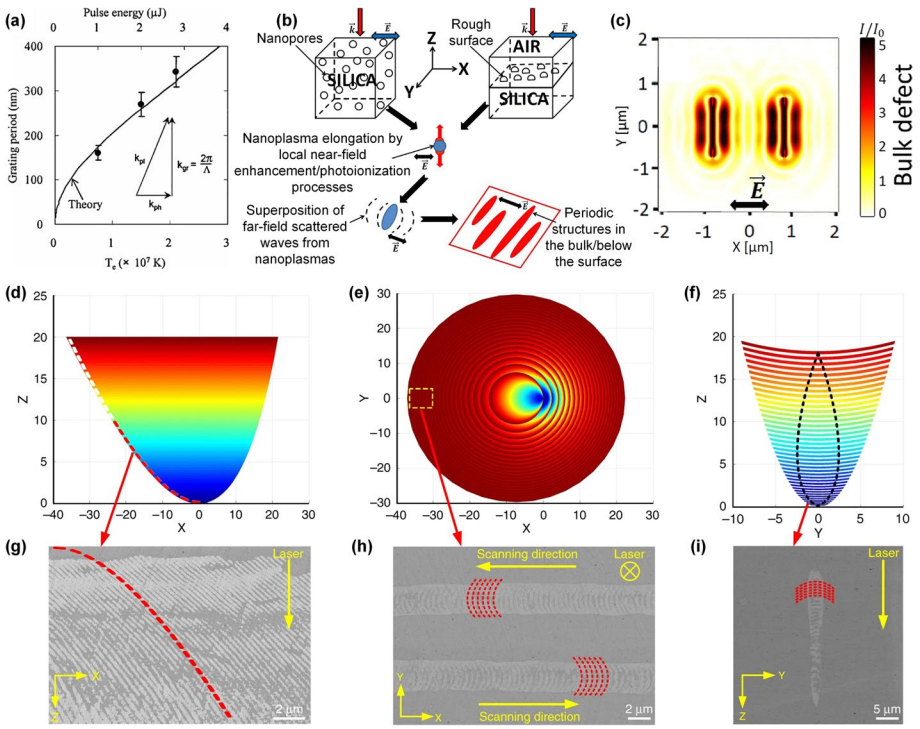


**Fig. 5** **a** Nanograting period evolution based on the plasma interference model [72]. Copyright 2003, American Physical Society. **b** Schematic of nanopore-mediated interference mechanisms for describing periodicity formation in bulk and on surfaces. **c** Secondary field modulation induced by the coherent superposition of the scattered waves from two adjacent nanoplanes [79]. Copyright 2017, Springer Nature. **d-f** Theoretically calculated 3D focal-area interference field presented by the equal-phase surfaces in d) XZ plane, e XY plane, and f YZ plane. **g-i** Corresponding SEM images of the actually produced structures by ULSN [78]. Copyright 2021, Springer Nature

scattered waves from different scattering centers enables a further reduction of the initial period, leading to the subwavelength periodicity (Fig. 5(c)) [79]. These models reasonably explain the polarization-dependence and multi-pulse accumulation-driven structure creation of nanogratings [110, 140], which promotes the maturity of interference-based models.

For new types of ULSN phenomena, the establishment and discussion of theoretical models are still rarely reported. In 2021, Zhang et al. [78] presented an extraordinary periodic crystallization structure in the LTN glass system that is polarization-independent but direction-dependent. This nanograting tilts opposite to the laser scanning direction and possesses a curved spatial morphology, which subverts the conventional understanding of the nanograting formation mechanism based on the interference model discussed above. To clarify this puzzle, the group proposed a brand new interference model where a single scattering center is introduced to replace the randomly distributed ionization centers or plasmas. According to this model, the interference is established by the scattered spherical waves from the scattering center and oblique incident waves that are distributed at the periphery of the focused beam (Fig. 5(d)-(f)). This model can quantitatively describe the intensity distribution of the interference field and the theoretically calculated result is in good agreement with the experimentally generated structures (Fig. 5(g)-(i)). They further demonstrated that this model is highly universal and can explain a series of similar ULSN phenomena not only in glasses but also in crystals. This study further extended the conventional interference model and greatly expand the application scope of this theory, which lays the foundation for further manipulating and utilizing different types of self-organized periodic structures. Notably, the interference model proposed here is conceptually different from the previous ones for explaining polarization-dependent nanogratings, which is reflected in the interference excitation, the scattering source, and the spatial morphology of the interference. In this model, the interference field is actively excited by ultrafast laser irradiation without relying on intrinsic defects or inhomogeneities in the glass network where the scattering field originates from the spherical light waves emitted by a single scattering center in the focal area rather than multiple inhomogeneous scattering centers or plasma waves. In addition, the spatial morphology of the interference field here is highly regular and strictly defined by the interference equations, rather than depending on ambiguous evolution processes.

With the deepening of research, the framework of the interference model for explaining early ULSN phenomena has become much clearer than before. However, with the discovery of new self-organized structures in multiple transparent media, plenty of disagreements and contradictions have been emerging in various branches of this theory. So far, different types of interference models are still largely isolated, and a highly general physical model that can offer a full understanding of ULSN has not yet been obtained. Therefore, more efforts need to be invested to disentangle the interrelationships and commonalities of different concepts to achieve a more refined and comprehensive theory.

### Plasma-based model

Bhardwaj et al. [141, 142] proposed a nanoplasmonic model to explain the ultrafast laser-induced periodic modifications in transparent dielectrics where the local field enhancement effect at the boundary of the initially sphere-shaped nanoplasmas causes an asymmetric growth in the orientation perpendicular to the laser polarization and form disk-shaped plasmas (Fig. 6(a)). During laser irradiation, these disk-shaped plasmas will become quasi-metallic and interact with subsequent incident light waves, which results in the periodic modulation of the plasmas and finally creates periodically assembled nanoplanes (Fig. 6(b)). According to this model, the regularly arranged nanoplanes will first form at the top of the irradiation volume and eventually fill the whole laser-modified area, and the period of these nanoplanes is estimated to be about λ/2n where λ is the ultrafast laser wavelength and n is the refractive index of the medium. This model provides a picture of the structural evolution process of ultrafast laser-induced periodic self-organization under multi-pulse interaction.

Liao et al. [77] presented that the standing plasma waves excited at the interfaces between modified and unmodified zones play an important role in the formation of

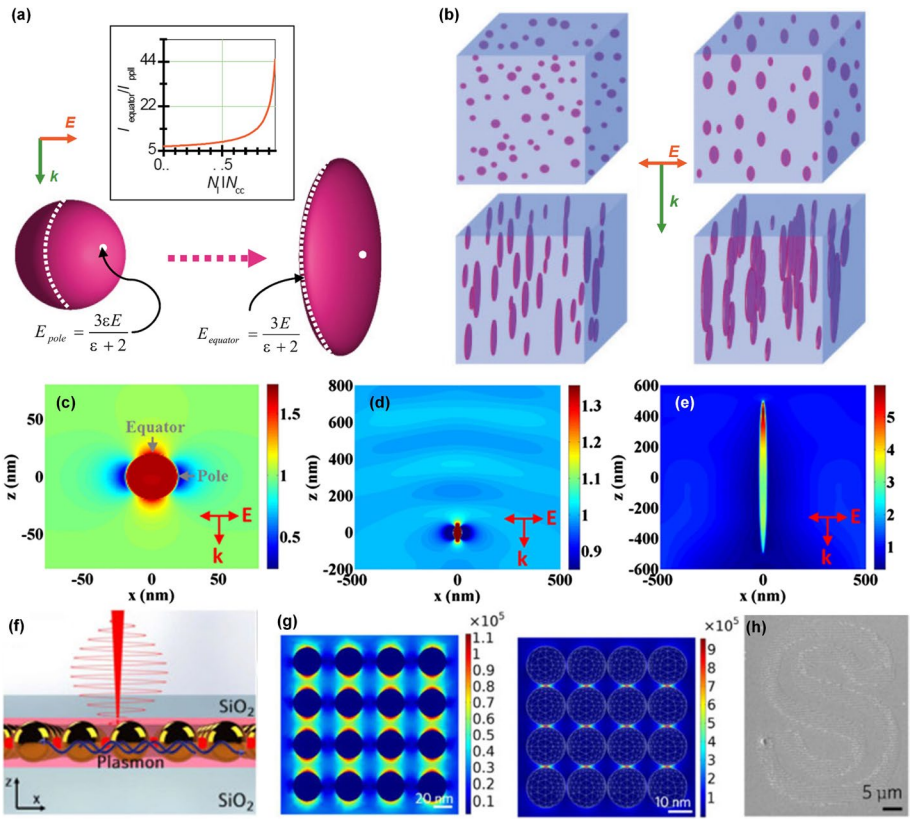


**Fig. 6** **a** Evolution mechanism of nanoplasmas based on asymmetric field enhancement and **b**) scheme of evolution of nanoplasmas into nanoplanes [90]. Copyright 2008, Wiley–VCH. **c-e** Theoretical distribution of light-filed intensity in XZ plane near **c**) a spherical nanoplasma, **d** an elliptical nanoplasma, and **e** an elliptical nanoplasma with a larger ellipticity [77]. Copyright 2015, Optica Publishing Group. **f** Schematic of ULSN in fused silica with ion-implanted Ag NPs. **g** Simulated electric field distribution for 15 nm (left) and 1 nm (right) spaced NPs. **h** SEM image of the letter "S" formed by self-assembled grating structures [136]. Copyright 2023, Elsevier

nanogratings by periodically modulating the electronic field intensity to excite nanoplasmas and induce periodic nanopores. According to this study, local field enhancement initially occurs at the equator of spherical nanoplasmas perpendicular to the polarization direction (Fig. 6(c)), which will induce an asymmetric ablation and thus lead to the formation of elliptical nanoplasmas. They also presented that the field enhancement occurs at the tips of elliptical nanoplasmas with different ellipticities (Fig. 6(d) and (e)), which further promotes the anisotropic growth of nanoplasmas and drives the nanopores to evolve into nanogratings with the increase of incident laser pulses. This interface-mediated mechanism is similar to that of ultrafast laser-induced surface ripples and explains many similarities between nanogratings and surface periodic structures. Notably, ultrafast laser-induced standing plasma waves are also used to interpret the formation of self-organized nanovoids in transparent dielectrics [143], which indicates the intercommunity of the formation mechanism of different ULSN-produced structures. In 2015, Liao et al. [144] further demonstrated that the coherent superposition of the scattering waves from early-formed nanogratings will create secondary optical intensity maxima. Such a local field enhancement is generally created between two nanoplanes and leads to the birth of new "son" nanoplanes, which explains the period reduction of nanogratings under the incidence of a large number of ultrafast pulses. Recently, Wu et al. [136] proposed a plasmon-enhanced ULSN by using ion implantation techniques (Fig. 6(f)). In this study, Ag ions are injected 100 nm below the surface and formed into homogeneous NPs in fused silica. Assisted by the significant light-field enhancement and localization of the NPs, the incident pulses excite and form a standing wave that can interfere with the subsequent laser pulses (Fig. 6(g)). This process enables establishing a periodic field distribution that drives the creation of subwavelength grating structures (Fig. 6(h)).

Plasma-based models are widely applied to describe the emergence and anisotropic growth of ultrafast laser-induced polarization-dependent periodic structures, such as the polarization-dependent nanopores [145], nanogratings [141], and nanoslits [146]. However, the lifetime of the light-excited electron plasma is only ~ 150 fs [147, 148], much shorter than the pulse interval of ultrafast laser, which limits the effectiveness of these models in explaining the subsequent interaction between nanoplasmas and incident waves. Thus, more in-depth works are still needed to clarify the bridging process from plasma generation to the activation of ULSN and thus complete plasma-based models.

#### Defect-based model

To bridge the temporal gap between the previously excited state and subsequently incident pulses, Richter et al. [100, 149] proposed a defect-assisted nanostructuring model where the self-trapped excitons (STEs) and defects induced by an ultrafast laser play a critical role in the formation of nanogratings (Fig. 7(a)). They investigated the coupling mechanism between individual pulses by tuning the temporal pulse separation from 500 fs to several ms. Experiments indicate that STEs are formed after the initial nonlinear absorption of ultrafast laser pulses and decay to point defects in about 500 ps. For very short pulse separations, the STEs promote the absorption of the following incident pulses, increasing the coupling between laser pulses and the material. When the pulse

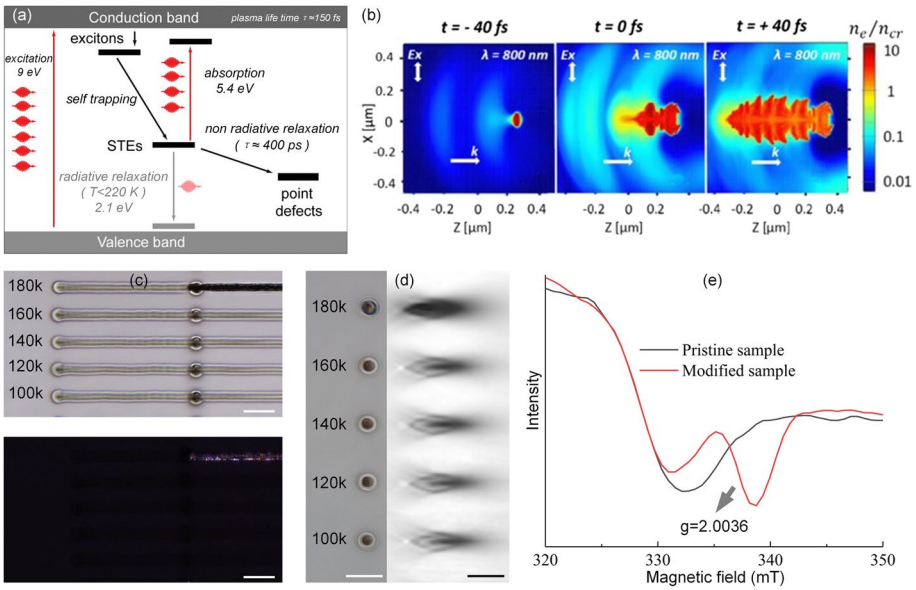


**Fig. 7** **a** Evolution process of STEs into point defects [100]. Copyright 2011, Laser Institute of America. **b** Evolution of electron density near a single inhomogeneity in glass [138]. Copyright 2016, American Physical Society. **c** Crystallite seeds assisted periodic crystallization test with different incident pulses and **d**) crystallite seed induction test with different incident pulses, and **e** EPR spectra of crystallite seeds and glass matrix [116]. Copyright 2021, Wiley–VCH

separation exceeds the lifetime of the STEs, the cumulative process of incident pulses is mediated by permanent defects.

Rudenko et al. [79, 138, 139] numerically investigated the formation mechanism of ultrafast laser-induced periodic structures in fused silica. According to their simulation, randomly distributed inhomogeneities in the material play an important role in forming scattering centers, creating different types of nanogratings, and tuning the nanograting period (Fig. 7(b)). Notably, these models are established mainly relying on the inherent defects or inhomogeneities in the fused silica and its universality in more other transparent dielectrics remains to be examined. In 2021, Zhang et al. [116] first reported a defect-assisted periodic crystallization in unconventional glasses where an auxiliary effect originates from photo-induced defects plays a decisive role (Fig. 7(c)). It is shown that the pre-irradiation of the medium with an ultrafast laser can locally induce defective crystallite seeds that can provide a unique domino-like assisting effect to activate and maintain continuous periodic phase transitions (Fig. 7(d)). The working principle of this auxiliary effect is to greatly reduce the pulse number and energy threshold for triggering ULSN process. Especially, the pulse density threshold can be reduced to 21–150 pulse/μm, nearly 10,000 times lower than that for inducing local crystallization by static laser irradiation. Electron paramagnetic resonance (EPR) measurement indicates that this auxiliary effect essentially originates from the laser-induced hole-trapped defect centers in the glass networks (Fig. 7(e)). Experiments also show that this mechanism is highly universal in multiple glass systems. This study sustains that ULSN process can be activated by the actively excited defects and changes the conventional concept that ULSN process relies on the intrinsic defects and heterogeneity of the matrix. The proposed model is especially suitable for explaining the continuous phase transition-typed ULSN phenomena in transparent dielectrics, which further extends the defect-based ULSN mechanisms.

Although many studies have confirmed the important role of various types of defects in mediating ULSN processes, the effectiveness of proposed models largely depends on the materials and experimental conditions. Consequently, there is still on consensus on the nature of these defects, specifically, where they come from, what they are, or how they work. In the next stage, more work is needed to clarify the spatiotemporal characteristics of the defects-assisted energy deposition and explore the defect-mediated ULSN in more different transparent dielectrics other than fused silica, including various unconventional glasses and crystals, to further complete the theory.

### Model improvements

Beam properties also play an important role in creating and manipulating structures during ULSN process. One important model is the pulse intensity forward tilt (PFT)-based ULSN. In 2012, Dai et al. [150] reported a controllable 3D-spatial rotation of the nanogratings in fused silica and proposed that this rotation depends on the angle between the PFT and the laser polarization direction (k). Specifically, PFT introduces an angle between the Poynting vector (p) and the wave vector, which decomposes the incident electric field into two electric field components perpendicular ($E_{\perp}$) and parallel ($E_{\parallel}$) to the laser propagation direction. The electric field component $E_{\perp}$ determines the orientation of nanogratings in the plane perpendicular to the laser propagation direction, while the electric field component $E_{\parallel}$ makes nanogratings rotate in the plane parallel to the laser propagation direction (Fig. 8(a)). According to this mechanism, an

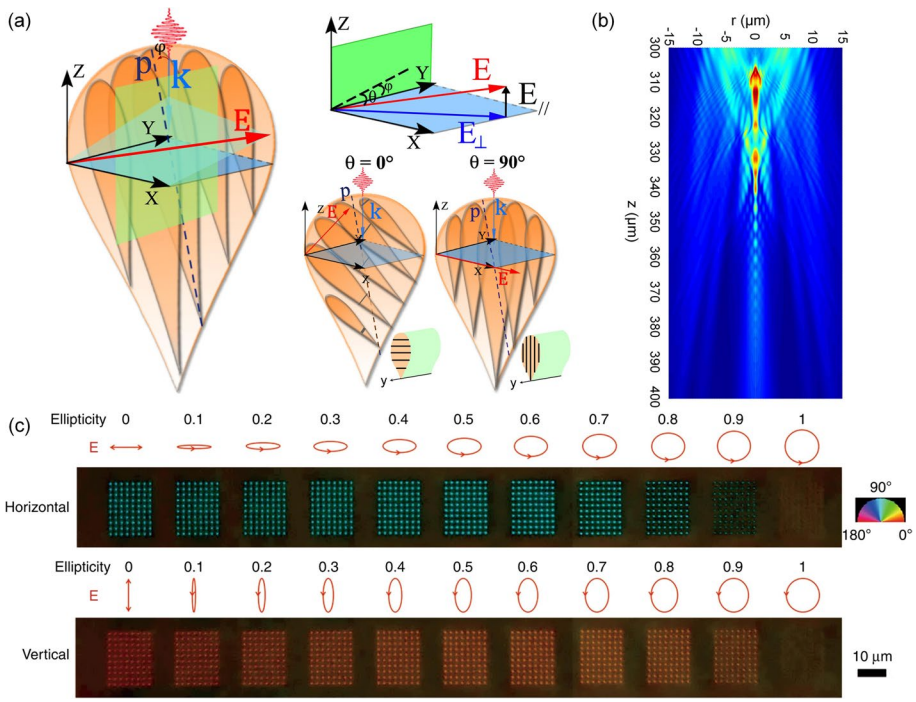


**Fig. 8** **a** Schematic of PFT-based 3D structural manipulation of nanogratings [150]. Copyright 2012, Optica Publishing Group. **b** Theoretically calculated fluence distribution at the focus [118]. Copyright 2008, AIP Publishing. **c** Birefringence images of imprinted nanopore-voxels. Pseudo colors show the orientation of the slow axis [151]. Copyright 2023, Springer Nature

ultrafast laser beam with PFT can be applied to simultaneously rotate nanogratings on two orthogonal planes and thus manipulate ULSN in 3D space [150].

Another representative example is the creation of self-organized periodic nanovoids where Gauss–Bessel beam [152], truncated Gaussian beam [122], and tightly focused Gaussian beam [117] were widely applied to achieve this class of ULSN. In the modeling, these beams are generally set as incident fields and combined with different light propagation and light-matter interaction models to obtain the theoretical fluence distribution. For example, Gaizauskas et al. [152] applied a zero-order Gauss-Bessel beam as the incident field to calculate the fluence distribution by using the nonlinear Schrodinger equation neglecting the plasma defocusing effect. The periodicity of the calculated fluence is similar to the experimentally induced structure. Mauclair et al. [122] applied a truncated Gaussian beam as the incident field and simulated the light field in the focal region by using the Fresnel linear propagation formalism. It was found that a series of fluence peaks appeared before the main focus, agreeing well with their experimental results. In 2008, Song et al. [118] took a tightly focused Gaussian beam as the incident field and proposed a composite model by combining the ultrafast laser nonlinear propagation model with the spherical aberration effect caused by the interface of two media with different refractive indices. Specifically, they applied a spherical aberration theory to obtain the light field after passing through the interface and set this light field as a new incident field, and then the fluence distribution in the medium is solved by incorporating the nonlinear Schrodinger equation and the electron density evolution equation (Fig. 8(b)). Their model and corresponding experimental results demonstrated the interface spherical aberration effect caused by the refractive index mismatch between air and the medium is the main reason for the ULSN creation of periodic nanovoids by a tightly focused ultrafast laser.

Recently, Lei et al. [151] observed that ULSN with an elliptically polarized beam in silica glass can create anisotropic nanopores whose birefringence signal intensity is about twice that induced by a linearly polarized beam, where the maximum birefringence is created by the elliptically polarized beam with an ellipticity of 0.6 (Fig. 8(c)). This is counterintuitive because the nonlinear absorption of an elliptically polarized ultrafast laser by fused silica is much weaker than that of a linearly polarized one. They attributed this abnormal phenomenon to the enhanced interaction of circularly polarized ultrafast laser with randomly oriented bonds and hole polarons in the glass network, and the high-efficiency ULSN creation of this birefringent structure can be interpreted as the result of a balance between the maximum concentration of nanopores at circular polarization and their anisotropic shaping driven by the linear polarization component.

To sum up, these studies discussed above further expand and refine the important roles of beam properties, interference, plasmas, and defects in ULSN process, and also illustrate the complexity of ULSN in transparent dielectrics, because there are cooperative effects between different models and various external factors. For example, the presence of nanostructures, optical aberration, and defects may affect the excitation and modulation of optical fields and also affect the role of beam polarization states in ULSN, which requires greater efforts in the future to gain a deeper understanding of how these mechanisms work together to activate and manipulate ULSN processes in different types of media.

## Applications based on ultrafast laser-induced self-organization in transparent dielectrics

As a high-resolution volume optical processing tool, ULSN is highly effective in creating complex all-inorganic mico-nano structures in various transparent dielectrics, which greatly enhances people's ability to construct integrated elements with ultrahigh stability, lifetime, and robustness. In recent years, more and more ULSN-based applications have been demonstrated in different functional materials. Here, we focus on representative research progress, including micro-nano optical elements, multidimensional data storage, and super-resolution etching, and briefly introduce some emerging novel applications.

### Micro-nano optical elements

In 2002, Bricchi et al. [153] demonstrated a birefringent Fresnel zone plate in silica fabricated by using ULSN (Fig. 9(a)), which is considered the earliest optical application based on ULSN methods. Since then, various intriguing micro-nano optical elements have emerged by using ULSN approaches (Fig. 9(b) and (c)), such as wave plates

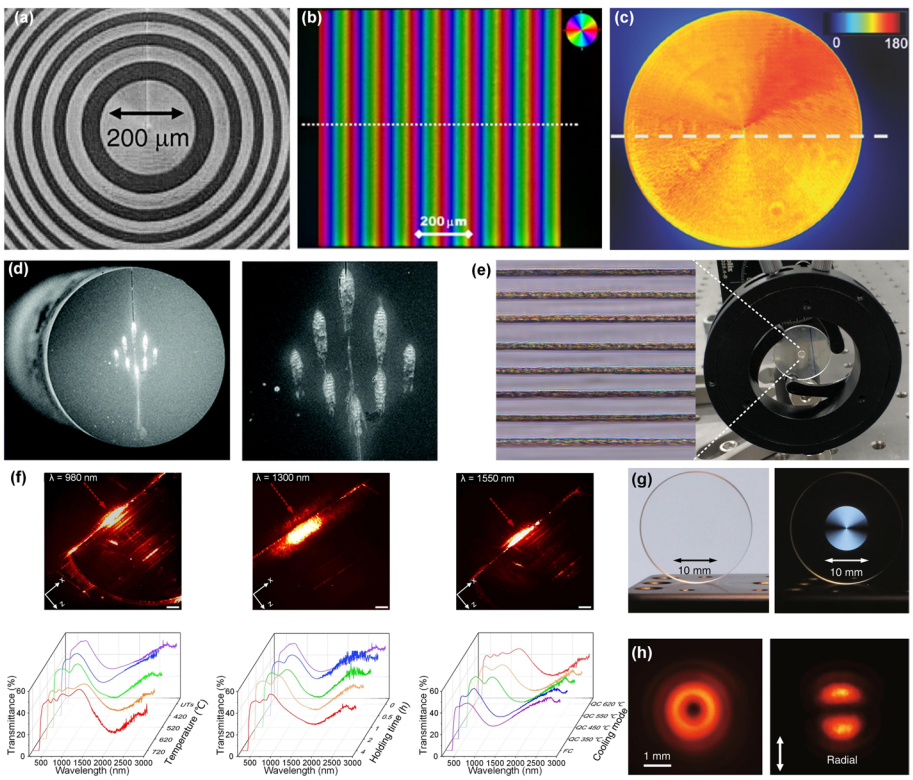


**Fig. 9** **a** Fresnel zone plate made of nanogratings in fused silica [153]. Copyright 2002, Optica Publishing Group. **b** Polarization diffraction gratings made of nanogratings in fused silica [157]. Copyright 2010, Optica Publishing Group. **c** Optical vortex converter made of nanogratings in $GeO_2$ glass [166]. Copyright 2017, Wiley–VCH. **d** In-line polarizer made by inscribing nanogratings in a single mode fiber [169]. Copyright 2019, Royal Society of Chemistry. **e** Near-infrared light attenuator made of periodic crystallization induced in LTN glass [115]. Copyright 2019, Wiley–VCH. **f** Tunable photonic crystal fabricated by ULSN-induced periodic crystallization [78]. Copyright 2021, Springer Nature. **g** Ultralow-loss polarization convertor made of self-organized nanopores in fused silica and **h**) corresponding beam conversion results [127]. Copyright 2020, Springer Nature

[154–156], polarization diffraction gratings [157], polarization selective holograms [158], light attenuators [115, 159, 160], Bragg gratings [161–164], and polarization converters [165–167]. Most of these applications are based on nanogratings in glasses due to a relatively complete understanding of the physicochemical characteristics and formation mechanisms of this structure [168]. Recently, with the expansion of application scenarios and the discovery of different types of self-organization phenomena, more pioneering applications emerge and greatly accelerate the maturing of ULSN.

Fiber is among the greatest innovations of human beings and provides an excellent platform for next-generation high-performance communication, sensing, measurement, and computing technologies [170]. Recently, ULSN-based fiber optics is fast developing to become a hot research field [171]. In 2019, Lu et al. [169] combined ULSN with fiber optics and first induced self-organized fiber nanogratings (FNGs) by ultrafast laser direct writing in a single mode silica fiber (Fig. 9(d)). In this work, an in-line polarizer is demonstrated based on FNGs, boosting the application of ULSN in all-fiber polarization mode control and high-order vector mode selection. In 2021, Wang et al. [172] demonstrated distributed fiber optical sensors by continuously inscribing FNGs in silica fiber core point by point. The insertion loss of single point sensor element can be as low as 0.001 dB and due to the excellent heat resistance of nanogratings, the fabricated fiber sensors can sustain long-term stability in high temperatures up to 1000 ℃. Notably, this study first demonstrated the application of FNGs based sensors in nuclear reactors, confirming the great potential of ULSN in fabricating robust optical devices for extreme environments.

In recent years, new types of ULSN-produced modifications have sprung up and remarkable progress has been made in practical applications. In 2019, Zhang et al. [115] presented a polarization-dependent light attenuation effect of the periodic crystallization in LTN glass system and demonstrated that a broadband light attenuator made of the periodic crystallization can work in the near-infrared region (Fig. 9(e)). This is the first report on the periodic crystallization-based optical application. In 2021, they further uncovered the dual optical modulation capability of periodic crystallization, including polarization-dependent light attenuation and wavelength-dependent selective optical transmittance [78]. Based on this, they further inscribed a multi-functional all-inorganic photonic crystal in the glass (Fig. 9(f)). Notably, by engineering a reversible secondary-phase transition of the crystal part in the periodic crystallization structure, the optical modulation performances of this photonic crystal can be broadly manipulated, which shows the excellent flexibility of ULSN-produced all-inorganic optical elements.

In 2020, Sakakura et al. [127] demonstrated geometrical phase optical elements based on ULSN-produced polarization-dependent nanopores in fused silica, such as geometrical phase prism, lens, and polarization convertor (Fig. 9(g) and (h)). Compared with the nanograting-based optical elements, the nanopore-based optical elements have an extremely high optical transmittance of about 99% in the visible and near-infrared waveband and higher than 90% even in the ultraviolet range, which is attributed to the ultralow scattering loss of the nanopores. In 2021, Xu et al. [131] inscribed periodic structures in sapphire and demonstrated the application of geometric phase elements, including geometric phase lens and Q-plate. These optical elements are demonstrated to

possess high imaging and focusing performances which may find applications in various harsh environments, such as high-power optics.

Although these newly presented ULSN technique routes are still in the early stage of investigation, they have already shown remarkable advantages in fabricating all-inorganic optical elements with excellent integration, robustness, flexibility, and high transmittance in 3D space. To give full play to these advantages, normalized and quantitative fabrication processes aiming for ULSN is needed to be established and completed to improve the regularity of the self-organized structures. And more potential application scenarios related to optical sensing, displaying, imaging, precision measurement, and signal processing are waiting for further exploration.

#### High-density data storage

With the rapid development of big data and artificial intelligence technologies, the amount of data generated by human society has been fast exploding [173–175]. Faced with the long-term ultra-large-scale data storage, currently applied technologies inherently have many drawbacks such as insufficient reliability, limited lifespan, and low storage density, resulting in considerably huge energy consumption [176–178]. If people continue to rely on conventional technologies, it will further exacerbate the global energy shortage. Therefore, there is an ever-urgent demand to develop long-term, energy saving, and high-density data storage technologies.

The erasable and rewritable polarization-dependent birefringence properties of nanogratings make this structure highly favorable for high density data storage. In 2008, Taylor et al. [90] demonstrated the in situ information rewriting based on the nanograting structures in fused silica where data voxels are effectively rewritten by following pulses with new polarization angled 45° to the initial one. In 2010, Shimotsuma et al. [179] demonstrated five-dimensional (5D) optical data storage by introducing the optical retardance and the azimuth angle of the slow axis of nanogratings as information multiplexing channels on the basis of XYZ spatial coordinates (Fig. 10(a)) whose storage density can be as large as 300 Gbit/cm$^3$, about 10 times as that of a 12 cm BlueRay disk. In 2015, Zhang et al. [180] characterized the lifetime of nanograting-based 5D optical data storage by thermally accelerated aging measurements. According to Arrhenius law, the room temperature decay time of nanogratings can be as long as $\sim 3 \times 10^{20}$ years (Fig. 10(b)), implying that the theoretical lifetime of the nanograting-based 5D optical data storage in fused silica is comparable to the age of the Universe, namely, an unlimited data storage lifetime.

However, as the formation of nanogratings in transparent dielectrics generally requires multi-pulses incidence, the recording speed of the nanograting-based data storage is limited by the incident pulse number per unit time. Besides, the pulse energy for nanograting creation is considerably high and the readout accuracy remains not enough, which is unfavorable for developing low-power data storage. Recently, Yan et al. [181] proposed a quasi-single-pulse approach to generate anisotropic nanostructures with birefringence properties in fused silica that allow high-speed data recording. In their proposal, the anisotropic nanostructure is induced by the spatiotemporal manipulation of a picosecond laser. The temporal manipulation is achieved by a beam splitter or a birefringence crystal that can split a single ultrafast pulse into two pulses. The spatial manipulation is achieved

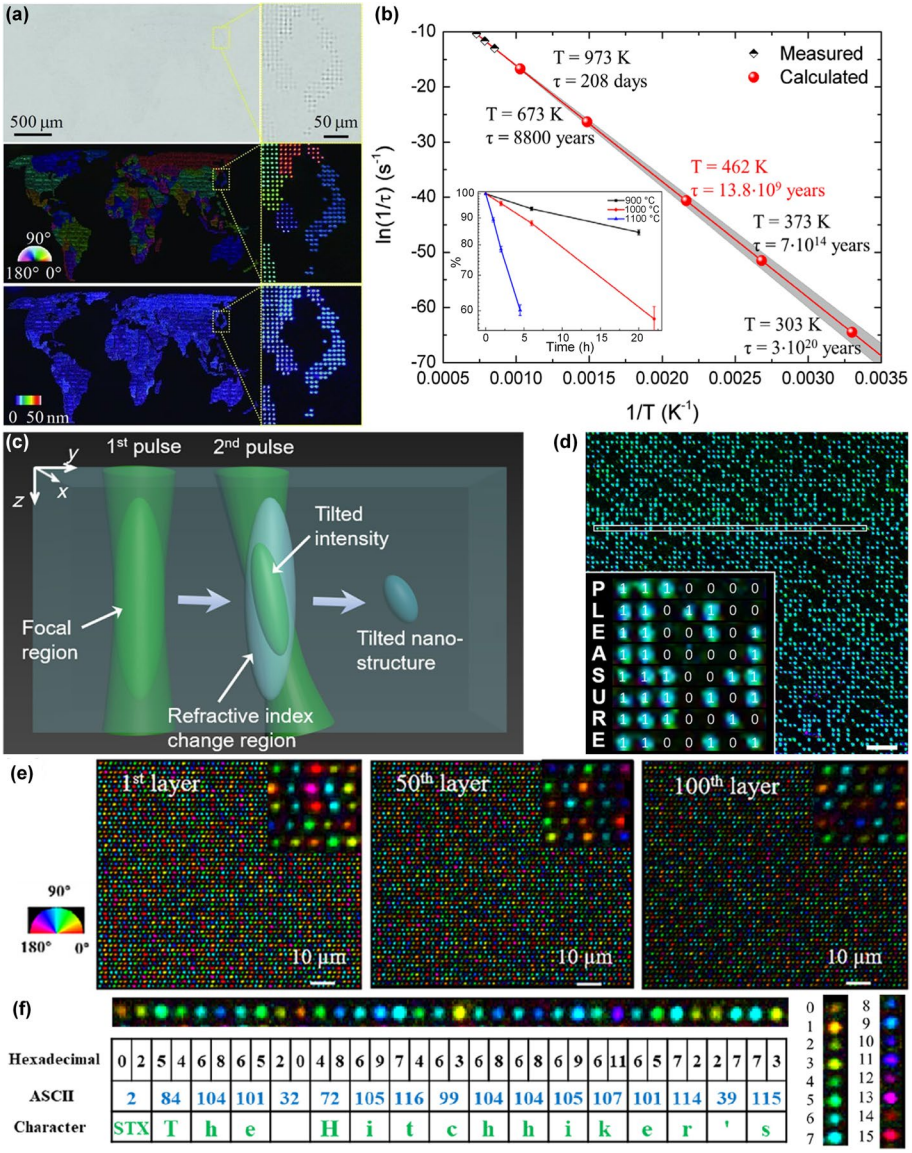


**Fig. 10** **a** 5D optical data storage with nanogratings in fused silica, including XYZ coordinates (up), slow axis orientation (middle), and optical retardance (below) [179]. Copyright 2010, Wiley–VCH. **b** Theoretical nanograting decay times at certain temperatures [180]. Copyright 2015, American Physical Society. **c** Schematic of formation mechanism of tilted anisotropic nanostructure and **d**) corresponding decoded data [181]. Copyright 2021, Optica Publishing Group. e 100-layer optical data storage with nanopores in fused silica [182]. Copyright 2022, Wiley–VCH. **f** Energy-efficient data storage with nanovoids induced by near-field enhancement effect [145]. Copyright 2021, Optica Publishing Group

by an SLM device that can dynamically manipulate the relative location of the first pulse and second pulse. The first pulse is used to excite STEs to induce a temporary high absorption and positive refractive index change. Then the second pulse partly interacts with the pre-modified area, creating a tilted intensity distribution, which is the origin of the anisotropic nanostructure (Fig. 10(c)). The readout accuracy of the written information can be up to 99.09% (Fig. 10(d)). Wang et al. [182] reported a high capacity multilayer 5D optical data storage based on ultrafast laser-induced polarization-dependent

nanopores that can greatly reduce the scattering loss of light. Benefitting from the high transmittance (99%), the readout accuracy of this multi-layer data storage can be considerably high. As proof, they demonstrated the recording of "The Hitchhiker's Guide to the Galaxy" into 100 layers of birefringent voxels in fused silica and the readout accuracy is examined as high as 100% (Fig. 10(e)). Lei et al. [145] demonstrated a fast and energy-efficient data recording approach by near-field enhancement mediated energy deposition manipulation. There, an isotropic circular nanovoid (~130 nm) is first induced by seeding pulses with pulse energy higher than the micro-explosion threshold and an anisotropic nano lamella-shaped structure (~460 nm) is then created by low-power writing pulses via the near-field enhancement effect (Fig. 10(f)). In the data recording, the incident pulse train consists of one seeding pulse (30 nJ) and seven (13.5 nJ) writing pulses for high retardance (~3 nm) or one seeding pulse (24 nJ) and four (13.5 nJ) writing pulses for low retardance (~1 nm). The information writing speed can be 225 Kb/s ($6 \times 10^5$ voxels/s) and the readout accuracy is examined at 99.5% and 96.3% for the top layer and the bottom layer (50 layers).

In summary, multiple types of ULSN-produced structures have shown great potential in developing next-generation optical storage technologies with considerably high data density, readout accuracy, and storage lifetime. However, current ULSN-based multi-dimensional data recording largely relies on multi-pulse incidence or seed pulse pre-modification in fused silica, which greatly limits the data writing speed. Besides, the optical setups for multi-dimensional information readout are too complex and bulky to satisfy the requirements of commercial applications. Therefore, real single pulse data recording routes still need to be exploited, where new storage media, data writing/readout mechanisms, algorithms for fast data extraction, and especially the miniaturization of memory systems are waiting for further investigation.

#### Micro-nano fluidic devices

The rapid development of ULSN greatly boosts the field of advanced manufacturing. Especially, ultrafast laser micromachining in transparent media produces various types of material modifications, such as defects, refractive index changes, cracks/voids, and so forth. By utilizing the unique physicochemical properties of the ULSN-modified area, on-demand subtractive nanostructuring with higher resolution and controllability can be further achieved. One representative example is ULSN-assisted 3D fluidic channel fabrication in transparent dielectrics.

In 2013, Liao et al. [183] proposed a sub-50 nm nanostructuring approach based on ULSN-induced nanogratings in a homemade high-silicate $SiO_2$-$B_2O_3$-$Na_2O$ porous glass. There, the induced nanogratings are induced as polarization-dependent periodic hollow nanovoids in the porous glass. By fixing the laser polarization perpendicular to the scanning direction and reducing the pulse energy to a certain value (~60 nJ), a single central nanovoid elongated in the writing path with a width of ~37 nm can be solely induced (Fig. 11(a) and (b)). The single nanovoid can be connected into a continuous nano-channel by using a low laser writing speed of 5–10 μm/s and a post-annealing treatment is applied to collapse the inherent nanopores in the glass matrix. The fluidic functionality is confirmed by filling the nano-channels with an observable fluorescent dye solution. They further fabricated integrated micro-nano fluidic systems by simultaneously inscribing

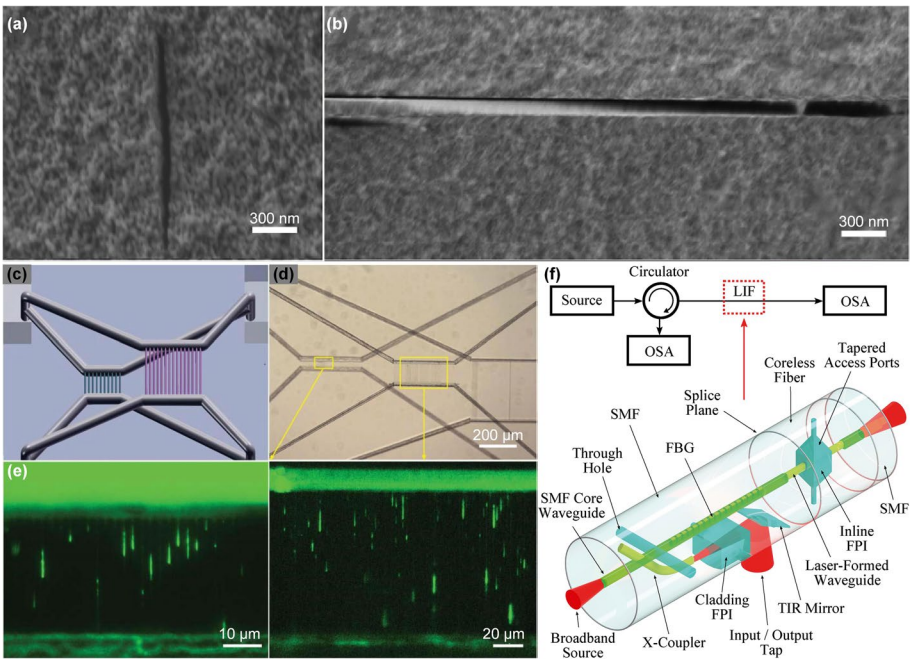


**Fig. 11** **a** Cross section and **b** top view SEM image of a single nanochannel induced in $SiO_2$-$B_2O_3$-$Na_2O$ porous glass by ULSN [183]. Copyright 2013, Optica Publishing Group. **c** Schematic and **d**) top-view optical image of 3D fluidic systems for DNA analysis, and **e**) fluorescent images of DNA stretching in nanochannels [184]. Copyright 2013, Royal Society of Chemistry. **f** Schematic of integrated LIF optofluidic systems [185]. Copyright 2014, Royal Society of Chemistry

conventional micro-channels and ULSN-based nano-channels into 3D fluidic configurations in the glass matrix [184]. The micro-nano fluidic systems are demonstrated as lab-on-a-chip devices for deoxyribonucleic acid (DNA) analysis and the stretching behaviors of DNA molecules are clearly observed in the nano-channels (Fig. 11(c)-(e)), opening up new approaches for the investigation of single molecular behaviors.

Recently, ultrafast laser-assisted subtractive fabrication has developed to become an effective tool for structuring all-inorganic transparent dielectrics in 3D by utilizing the great etching rate difference in chemical etchants of the irradiated and unirradiated zones [186–189]. ULSN process has been confirmed to possess multi-dimensionally controllable super-resolution material modification abilities that are well suited for higher precision etching in transparent dielectrics, namely, ULSN-assisted etching. Hnatovsky et al. and Cheng et al. [91, 97, 190, 191] systematically studied the selective etching properties of nanogratings in glasses and revealed the highly differential etching rate inside nanogratings, which lays the foundation for ULSN-assisted microfluidic channel fabrication. Haque et al. [185] further combined ULSN-assisted etching and ultrafast laser 3D structuring inside optical fibers to construct highly integrated lab-in-fiber (LIF) optofluidic systems that consist of various microfluidic channels and optical resonators (Fig. 11(f)). The fabricated LIF devices are demonstrated to possess broad prospects in in-line bend, strain, refractive index, and temperature sensing.

ULSN-assisted micro-nano fabrication provides a facile and powerful approach for constructing advanced micro-fluidic devices. However, current studies largely focus on structure minimizing and efficiency improvement. There are still research gaps in

on-demand channel shape control, inner-surface engineering, and modular integration of micro-fluidic systems. With the advent of various new types of ULSN phenomena, mechanisms, and materials, more novel ULSN-assisted micro-nano fluidic technologies aiming for fields like personalized medicine, fast virus detection, and efficient microreactors, are expected to be new hotspots in this field.

### Other applications

In addition to the classic applications, some intriguing ULSN-based applications have also begun to sprout in recent years, providing new insights into frontier fields like extreme fabrication, structural coloration, and chiral optics.

For example, Yan et al. [146] proposed a direct optical nanofabrication approach that enables 3D processing in fused silica with a considerably high spatial resolution down to 40 nm and a lateral spacing down to 200 nm. This technology is based on the creation of a polarization-dependent single nanoslit structure by using ULSN. Specifically, the laser polarization is set perpendicular to the scanning direction to activate the continuous growth of the structure along the writing path and thus form a high-aspect-ratio single nanoslit structure, where the near-field redistribution induced by the presence of the nanoslit allows for achieving a lateral spacing much smaller than the laser beam size. As a proof of concept, they demonstrated the fabrication of customized 3D nanostructures formed by nanoslits (Fig. 12(a)). This ULSN process can serve as a general

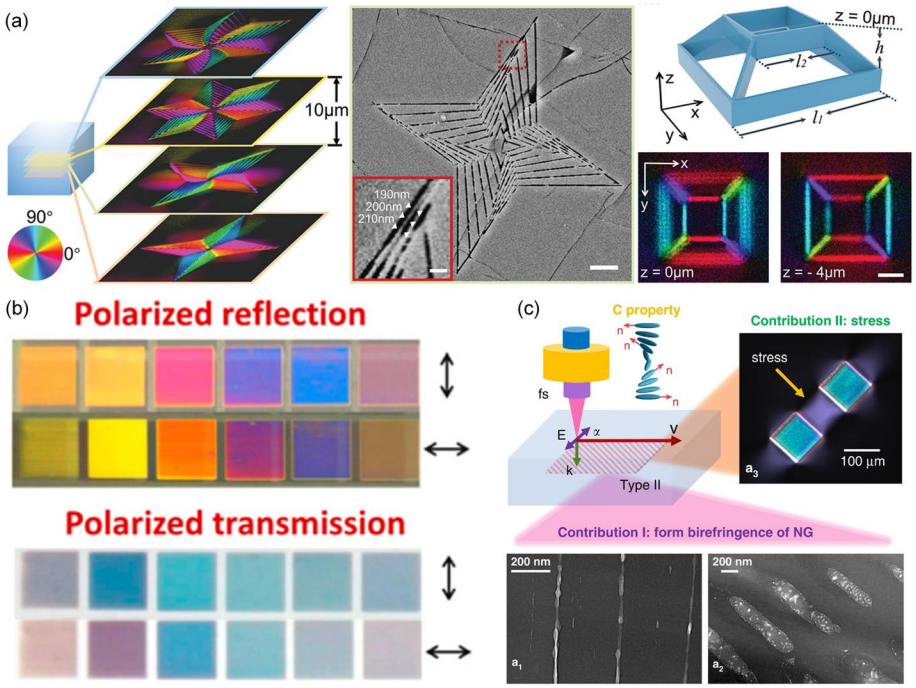


**Fig. 12** **a** 3D nanofabrication based on the ULSN creation of self-organized nanosilts, including nanopatterns in four layers (left), SEM image of the nanopattern in the third layer (middle), and truncated pyramid structure (right) [146]. Pseudo colors show the orientation of the slow axis. Copyright 2021, Wiley–VCH. **b** Polarization-sensitive color generated by grating structures in nanocomposite films [133]. Copyright 2017, American Chemical Society. **c** ULSN creation of nanogratings possessing circular properties [192]. Copyright 2023, Springer Nature

nanofabrication approach that is broadly applicable in constructing functional structures for nanophotonics, nanofluidics, nanomechanics, metamaterials, and information recording.

In 2017, Liu et al. [133] reported a novel coloration route based on ULSN-produced 3D metallic nanostructures in a nanocomposite thin film (Ag NPs: $TiO_2$). In this work, they presented that the irradiation of a linearly polarized ultrafast laser on the film can simultaneously excite two independent propagating optical modes (a surface mode and a guided mode) and both of these modes can interact with incident waves to establish periodic field distributions, leading to the creation of composite self-assembled nanostructures with two periodicities. By utilizing the diffractive and polarization-sensitive properties of the induced nanostructures, they demonstrated the high potential of this ULSN strategy in structural coloration and multiplexed optical image encoding (Fig. 12(b)). This work also prospected the potential of such nanostructured composite films in applications like solar energy harvesting, photocatalysis, and photochromic devices.

Recently, Lu et al. [192] reported the tailoring of chiral optical properties in 3D by ULSN in an initially achiral material (silica glass). In a simple view, they observed that there are two major contributions that ULSN-produced nanogratings own to its aggregate birefringent response, namely, a form and a stress-related one (Fig. 12(c)), and then respectively investigated the polarization-dependence properties of these two contributions and established a two-layer model based on Mueller formalism to describe the generation of chiral optical properties of the laser-modified area. Under the guidance of this model, they demonstrated two types of chiral optical elements, including nanograting-based waveplates and stress-based waveplates to achieve customized optical rotation. Predictably, the presented principle allows for flexibly designing 3D structured light beams in terms of phase, amplitude, and polarization, providing a novel perspective on tailoring the optical properties of transparent dielectrics.

Although still in their infancy, these studies are impressive enough to represent an important milestone in shaping ULSN into a highly flexible and versatile tool for promoting advanced material modification and light-matter interaction physics. However, many of the envisioned application scenarios in these reports are still to be implemented and a more exhaustive performance characterization of the corresponding devices or elements is required. Towards practical applications, more work is still required in the future to improve manufacturing efficiency, structural controllability, as well as the uniformity of mass production.

## Conclusions and outlook

ULSN in transparent dielectrics has made remarkable progress in creating a versatile platform for ultrafast laser-matter interactions and extreme material processing, giving birth to a large number of new phenomena, theoretical models, and engineering applications, which offers competitive solutions to many challenging problems in various multidisciplinary fields, including quantum technology, big data storage, advanced optical sensing, detecting, imaging, and communication. Predictably, ULSN will continue to be a hot research topic in strong-field physics in the future and bring us more fascinating discoveries.

In this review, we comb recent progress and key milestones in ULSN and ULSN-based technologies. Nanograting, as the most widely researched object, has established itself as an important mother structure for predicting and exploiting more ULSN approaches due to its highly general physicochemical characteristics. Excitingly, we note that a rising number of unprecedented phenomena have emerged in recent years one after another, and gradually developed into important branches of ULSN. Inspired by the formation mechanism of nanogratings, novel theories and physical models have been proposed to explain newly discovered ULSN phenomena and direct the structural manipulation, which is followed by a burst of pioneering applications based on these ULSN-produced structures. We excitingly witness a giant improvement in the performances of various elements and devices fabricated by ULSN, which benefits from the favorable properties of the created structures. However, the fast progress of ULSN is accompanied by plenty of conflicts and puzzles between new concepts and established theoretical frameworks. The specific roles of optical scattering, interference, and field enhancement effect in ULSN process are still controversial and the plasma and defect-mediated structural evolution process remain largely unclear. As a result, it is still far away from achieving a consensus on the essence of ULSN. In the future, advanced ultrafast dynamics detection approaches like pump-probe spectroscopy [193], ultrafast photography [194], and ultrafast electro-optical imaging [195] would be useful to provide more intuitive experimental evidence for different models and unravel these mysteries. Moreover, we have recently witnessed the booming of various optical modulation technologies, including super-resolution microscopy [196], adaptive aberration control [197], SLM [198], and optical parametric amplifier (OPA) [199], etc. We believe these technologies can serve as powerful tools during ULSN process to achieve much more flexible structural manipulation of the period, height, and uniformity of the self-organized structures in the near future.

The rapid expansion of technologies like data mining, machine learning, and artificial intelligence, has brought human society into the era of information on explosion. Light, as a powerful information carrier, represents the future of information technologies where transparent dielectrics provide a versatile platform for light manipulation. ULSN in transparent dielectrics offers a tremendously attractive brand new idea for artificially tailoring natural materials to realize on-demand manipulation of light at micro-nano scale. Therefore, the future orientation of ULSN would be the enabler for highly integrated optical information processing, transmission, and storage. Technically, the coupling between ULSN-produced micro-nano optical elements and commercial optoelectronic devices is desired to be optimized. Multifunctional integrated optical systems across materials and elements have not been effectively demonstrated by ULSN. In addition, standardized, efficient, and mass ULSN fabrication is urgently needed to be achieved. For ULSN-based multi-dimensional data storage, there is still significant space to improve the information recording and readout speed. Higher density data storage with more information multiplexing channels, such as light frequency and photon orbital angular momentum (OAM) [200–202], remains to be further explored by ULSN in transparent dielectrics. In addition, the data writing and reading systems are not integrated and facile enough for commercial use. Thus, more efforts are needed to be invested in solving these problems.

ULSN in transparent dielectrics has developed into a broad research field rather than a small subdivision. Therefore, future research should be systematic and intrinsically associated with physics, optics, material science, computer science, and mechanical engineering. It is exciting to combine ULSN with diverse frontier cross-disciplinary technologies to establish a family of universal multifunctional material modification methods that can freely manipulate ULSN processes and construct arbitrary geometries and complicated systems in arbitrary materials.

**Abbreviations**

| | |
|---|---|
| ULSN | Ultrafast laser-induced self-organized nanostructuring |
| 3D | Three-dimensional |
| RI | Refractive index |
| LTN | $La_2O_3$-$Ta_2O_5$-$Nb_2O_5$ |
| SEM | Scanning electron microscopy |
| HRTEM | High-resolution transmission electron microscopy |
| TEM | Transmission electron microscopy |
| NPs | Nanoparticles |
| STEs | Self-trapped excitons |
| EPR | Electron paramagnetic resonance |
| FNGs | Fiber nanogratings |
| 5D | Five-dimensional |
| DNA | DeoxyriboNucleic acid |
| LIF | Lab-in-fiber |
| SLM | Spatial light modulation |
| OPA | Optical parametric amplifier |
| OAM | Photon orbital angular momentum |

**Acknowledgements**
Not applicable.

**Authors' contributions**
Writing-original draft preparation: BZ, ZW. Writing-review and editing: DT, JQ. BZ was a major contributor in writing the manuscript. All authors read and approved the final manuscript.

**Funding**
This work was financially supported by the National Natural Science Foundation of China (Grant Nos. U20A20211, 51902286, 61905215, and 62005164); the National Key R&D Program of China (No. 2021YFB2800500); the Key Research Project of Zhejiang Lab; China Postdoctoral Science Foundation (2021M702799).

**Availability of data and materials**
The datasets and figures used and analyzed during the current study are available from the corresponding author on reasonable request.

## Declarations

**Competing interests**

The authors declare that they have no competing interests.

Received: 23 November 2022 Revised: 24 June 2023 Accepted: 12 July 2023
Published online: 25 July 2023

**References**

1. Wang X-J, Fang H-H, Sun F-W, Sun H-B. Laser Writing of Color Centers. Laser Photonics Rev. 2022;16:2100029. https://doi.org/10.1002/lpor.202100029.
2. Du Y, et al. Precipitation of CsPbBr 3 quantum dots in borophosphate glasses inducted by heat-treatment and UV-NIR ultrafast lasers. Chem Eng J. 2020;401:126132. https://doi.org/10.1016/j.cej.2020.126132.
3. Mizuochi N, et al. Electrically driven single-photon source at room temperature in diamond. Nat Photonics. 2012;6:299–303. https://doi.org/10.1038/nphoton.2012.75.
4. Jin D, et al. 22.5-W narrow-linewidth diamond Brillouin laser at 1064 nm. Opt Lett. 2022;47:5360–3. https://doi.org/10.1364/OL.471447.
5. Yu M, et al. Integrated femtosecond pulse generator on thin-film lithium niobate. Nature. 2022. https://doi.org/10.1038/s41586-022-05345-1.

6. Fang J, et al. 3D waveguide device for few-mode multi-core fiber optical communications. Photon Res. 2022;10:2677–85. https://doi.org/10.1364/PRJ.465174.
7. Wang P, Wang Y, Tong L. Functionalized polymer nanofibers: a versatile platform for manipulating light at the nanoscale. Light Sci Appl. 2013;2:102. https://doi.org/10.1038/lsa.2013.58.
8. Tan D, et al. Fabricating low loss waveguides over a large depth in glass by temperature gradient assisted femtosecond laser writing. Opt Lett. 2020;45:3941–4. https://doi.org/10.1364/OL.396861.
9. Xu P, et al. Elastic ice microfibers. Science. 2021;373:187–92. https://doi.org/10.1126/science.abh3754.
10. Zhang X-L, et al. Non-Abelian braiding on photonic chips. Nat Photonics. 2022;16:390–5. https://doi.org/10.1038/s41566-022-00976-2.
11. Li L, et al. Integrated flexible chalcogenide glass photonic devices. Nat Photonics. 2014;8:643–9. https://doi.org/10.1038/nphoton.2014.138.
12. Pelucchi E, et al. The potential and global outlook of integrated photonics for quantum technologies. Nat Rev Phys. 2022;4:194–208. https://doi.org/10.1038/s42254-021-00398-z.
13. Wang T, et al. Periodically poled LiNbO3 crystals from 1D and 2D to 3D. SCIENCE CHINA Technol Sci. 2020;63:1110–26. https://doi.org/10.1007/s11431-019-1503-0.
14. Zhu D, et al. Integrated photonics on thin-film lithium niobate. Adv Opt Photon. 2021;13:242–352. https://doi.org/10.1364/AOP.411024.
15. Juodkazis S, et al. Optical third harmonic generation during femtosecond pulse diffraction in a Bragg grating. J Phys D Appl Phys. 2006;39:50. https://doi.org/10.1088/0022-3727/39/1/009.
16. Dezhi T, Zhuo W, Beibei X, Jianrong Q. Photonic circuits written by femtosecond laser in glass: improved fabrication and recent progress in photonic devices. Adv Photonic. 2021;3:1–24. https://doi.org/10.1117/1.AP.3.2.024002.
17. Meany T, et al. Laser written circuits for quantum photonics. Laser Photonics Rev. 2015;9:363–84. https://doi.org/10.1002/lpor.201500061.
18. Sun K, et al. Three-dimensional direct lithography of stable perovskite nanocrystals in glass. Science. 2022;375:307–10. https://doi.org/10.1126/science.abj2691.
19. Chen F, de Aldana JRV. Optical waveguides in crystalline dielectric materials produced by femtosecond-laser micromachining. Laser Photonics Rev. 2014;8:251–75. https://doi.org/10.1002/lpor.201300025.
20. Zhang X-L, et al. Non-Abelian braiding on photonic chips. Nat Photonics. 2022. https://doi.org/10.1038/s41566-022-00976-2.
21. Pezzagna S, Meijer J. Quantum computer based on color centers in diamond. Appl Phys Rev. 2021;8:011308. https://doi.org/10.1063/5.0007444.
22. Lenzini F, Gruhler N, Walter N, Pernice WHP. Diamond as a Platform for Integrated Quantum Photonics. Adv Quantum Technol. 2018;1:1800061. https://doi.org/10.1002/qute.201800061.
23. Ams M, Marshall GD, Spence DJ, Withford MJ. Slit beam shaping method for femtosecond laser direct-write fabrication of symmetric waveguides in bulk glasses. Opt Express. 2005;13:5676–81. https://doi.org/10.1364/OPEX.13.005676.
24. Kowalevicz AM, Sharma V, Ippen EP, Fujimoto JG, Minoshima K. Three-dimensional photonic devices fabricated in glass by use of a femtosecond laser oscillator. Opt Lett. 2005;30:1060–2. https://doi.org/10.1364/OL.30.001060.
25. Marshall GD, et al. Laser written waveguide photonic quantum circuits. Opt Express. 2009;17:12546–54. https://doi.org/10.1364/OE.17.012546.
26. Sun Y-K, et al. Non-Abelian Thouless pumping in photonic waveguides. Nat Phys. 2022;18:1080–5. https://doi.org/10.1038/s41567-022-01669-x.
27. Crespi A, et al. Integrated photonic quantum gates for polarization qubits. Nat Commun. 2011;2:566. https://doi.org/10.1038/ncomms1570.
28. Crespi A, et al. Integrated multimode interferometers with arbitrary designs for photonic boson sampling. Nat Photonics. 2013;7:545–9. https://doi.org/10.1038/nphoton.2013.112.
29. Wang C-Y, Gao J, Jin X-M. On-chip rotated polarization directional coupler fabricated by femtosecond laser direct writing. Opt Lett. 2019;44:102–5. https://doi.org/10.1364/OL.44.000102.
30. Xu T, et al. Three-dimensional nonlinear photonic crystal in ferroelectric barium calcium titanate. Nat Photonics. 2018;12:591–5. https://doi.org/10.1038/s41566-018-0225-1.
31. Wei D, et al. Efficient nonlinear beam shaping in three-dimensional lithium niobate nonlinear photonic crystals. Nat Commun. 2019;10:4193. https://doi.org/10.1038/s41467-019-12251-0.
32. Wei D, et al. Experimental demonstration of a three-dimensional lithium niobate nonlinear photonic crystal. Nat Photonics. 2018;12:596–600. https://doi.org/10.1038/s41566-018-0240-2.
33. Ouyang X, et al. Synthetic helical dichroism for six-dimensional optical orbital angular momentum multiplexing. Nat Photonics. 2021;15:901–7. https://doi.org/10.1038/s41566-021-00880-1.
34. Wang Z, Tan D, Qiu J. Single-shot photon recording for three-dimensional memory with prospects of high capacity. Opt Lett. 2020;45:6274–7. https://doi.org/10.1364/OL.409171.
35. Gao L, Zhang Q, Evans RA, Gu M. 4D Ultra-High-Density Long Data Storage Supported by a Solid-State Optically Active Polymeric Material with High Thermal Stability. Adv Opt Mater. 2021;9:2100487. https://doi.org/10.1002/adom.202100487.
36. Sung JH, et al. 4.2 PW, 20 fs Ti:sapphire laser at 0.1 Hz. Opt Lett. 2017;42:2058–61. https://doi.org/10.1364/OL.42.002058.
37. Tan D, Sharafudeen KN, Yue Y, Qiu J. Femtosecond laser induced phenomena in transparent solid materials: Fundamentals and applications. Prog Mater Sci. 2016;76:154–228. https://doi.org/10.1016/j.pmatsci.2015.09.002.
38. Gattass RR, Mazur E. Femtosecond laser micromachining in transparent materials. Nat Photonics. 2008;2:219–25. https://doi.org/10.1038/nphoton.2008.47.
39. Huang X, et al. Reversible 3D laser printing of perovskite quantum dots inside a transparent medium. Nat Photonics. 2020;14:82–8. https://doi.org/10.1038/s41566-019-0538-8.
40. Guo B, et al. Femtosecond Laser Micro/Nano-manufacturing: Theories, Measurements, Methods, and Applications. Nanomanufacturing Metrol. 2020;3:26–67. https://doi.org/10.1007/s41871-020-00056-5.

41. Jia Y, Wang S, Chen F. Femtosecond laser direct writing of flexibly configured waveguide geometries in optical crystals: fabrication and application. Opto-Electronic Advances. 2020;3, 190042-190041-190042-190012, https://doi.org/10.29026/oea.2020.190042.
42. Lin Z, Hong M. Femtosecond Laser Precision Engineering: From Micron, Submicron, to Nanoscale. Ultrafast Science. 2021;2021:9783514. https://doi.org/10.34133/2021/9783514.
43. Tan D, Zhang B, Qiu J. Ultrafast Laser Direct Writing in Glass: Thermal Accumulation Engineering and Applications. Laser Photonics Rev. 2021;15:2000455. https://doi.org/10.1002/lpor.202000455.
44. Hu Y, Zhang W, Ye Y, Zhao Z, Liu C. Femtosecond-Laser-Induced Precipitation of CsPbBr 3 Perovskite Nanocrystals in Glasses for Solar Spectral Conversion. ACS Applied Nano Materials. 2020;3:850–7. https://doi.org/10.1021/acsanm.9b02362.
45. Eliezer S, et al. Synthesis of nanoparticles with femtosecond laser pulses. Physical Review B. 2004;69:144119. https://doi.org/10.1103/PhysRevB.69.144119.
46. Maximova K, Aristov A, Sentis M, Kabashin AV. Size-controllable synthesis of bare gold nanoparticles by femtosecond laser fragmentation in water. Nanotechnology. 2015;26:065601. https://doi.org/10.1088/0957-4484/26/6/065601.
47. Liu S-F, et al. 3D nanoprinting of semiconductor quantum dots by photoexcitation-induced chemical bonding. Science. 2022;377:1112–6. https://doi.org/10.1126/science.abo5345.
48. Yuan Y, et al. Ultrafast Shaped Laser Induced Synthesis of MXene Quantum Dots/Graphene for Transparent Supercapacitors. Adv Mater. 2022;34:2110013. https://doi.org/10.1002/adma.202110013.
49. Xing J-F, Zheng M-L, Duan X-M. Two-photon polymerization microfabrication of hydrogels: an advanced 3D printing technology for tissue engineering and drug delivery. Chem Soc Rev. 2015;44:5031–9. https://doi.org/10.1039/C5CS00278H.
50. Geng Q, Wang D, Chen P, Chen S-C. Ultrafast multi-focus 3-D nano-fabrication based on two-photon polymerization. Nat Commun. 2019;10:2179. https://doi.org/10.1038/s41467-019-10249-2.
51. Kotz F, et al. Two-Photon Polymerization of Nanocomposites for the Fabrication of Transparent Fused Silica Glass Microstructures. Adv Mater. 2021;33:2006341. https://doi.org/10.1002/adma.202006341.
52. Hua JG, Liang SY, Chen QD, Juodkazis S, Sun HB. Free-Form Micro-Optics Out of Crystals: Femtosecond Laser 3D Sculpturing. Advanced Functional Materials n/a, 2200255, https://doi.org/10.1002/adfm.202200255 (2022).
53. Fang Y, et al. Liquid-Infused Slippery Stainless Steel Surface Prepared by Alcohol-Assisted Femtosecond Laser Ablation. Adv Mater Interfaces. 2021;8:2001334. https://doi.org/10.1002/admi.202001334.
54. Balling P, Schou J. Femtosecond-laser ablation dynamics of dielectrics: basics and applications for thin films. Rep Prog Phys. 2013;76:036502. https://doi.org/10.1088/0034-4885/76/3/036502.
55. Yu L, et al. Nanochannels with a 18-nm feature size and ultrahigh aspect ratio on silica through surface assisting material ejection. Adv Photonics Nexus. 2022;1:026004. https://doi.org/10.1117/1.APN.1.2.026004.
56. Stone A, et al. Directionally controlled 3D ferroelectric single crystal growth in LaBGeO5 glass by femtosecond laser irradiation. Opt Express. 2009;17:23284–9. https://doi.org/10.1364/OE.17.023284.
57. Miura K, Qiu J, Mitsuyu T, Hirao K. Space-selective growth of frequency-conversion crystals in glasses with ultrashort infrared laser pulses. Opt Lett. 2000;25:408–10. https://doi.org/10.1364/OL.25.000408.
58. Stone A, et al. Formation of ferroelectric single-crystal architectures in LaBGeO5 glass by femtosecond vs. continuous-wave lasers. J Non-Cryst Solids. 2010;356:3059–65. https://doi.org/10.1016/j.jnoncrysol.2010.03.048.
59. Zheng Y, et al. Valence state manipulation of Sm3+ ions via a phase-shaped femtosecond laser field. Photon Res. 2018;6:144–8. https://doi.org/10.1364/PRJ.6.000144.
60. Qiu J, et al. Space-selective valence state manipulation of transition metal ions inside glasses by a femtosecond laser. Appl Phys Lett. 2001;79:3567–9. https://doi.org/10.1063/1.1421640.
61. Royon A, et al. Silver Clusters Embedded in Glass as a Perennial High Capacity Optical Recording Medium. Adv Mater. 2010;22:5282–6. https://doi.org/10.1002/adma.201002413.
62. Tokel O, et al. In-chip microstructures and photonic devices fabricated by nonlinear laser lithography deep inside silicon. Nat Photonics. 2017;11:639–45. https://doi.org/10.1038/s41566-017-0004-4.
63. Liu X-Q, et al. Biomimetic sapphire windows enabled by inside-out femtosecond laser deep-scribing. PhotoniX. 2022;3:1. https://doi.org/10.1186/s43074-022-00047-3.
64. Liu X-Q, Bai B-F, Chen Q-D, Sun H-B. Etching-assisted femtosecond laser modification of hard materials. Opto-Electronic Advances. 2019;2:190021–190021. https://doi.org/10.29026/oea.2019.190021.
65. Geng J, Yan W, Shi L, Qiu M. Surface plasmons interference nanogratings: wafer-scale laser direct structuring in seconds. Light. 2022;11:189. https://doi.org/10.1038/s41377-022-00883-9.
66. Li Z-Z, et al. O-FIB: far-field-induced near-field breakdown for direct nanowriting in an atmospheric environment. Light. 2020;9:41. https://doi.org/10.1038/s41377-020-0275-2.
67. Chen L, et al. Large-area straight, regular periodic surface structures produced on fused silica by the interference of two femtosecond laser beams through cylindrical lens. Opto-Electronic Advances. 2021;4, 200036–200031–200036–200039, https://doi.org/10.29026/oea.2021.200036
68. Yong J, Chen F, Yang Q, Jiang Z, Hou X. A Review of Femtosecond-Laser-Induced Underwater Superoleophobic Surfaces. Adv Mater Interfaces. 2018;5:1701370. https://doi.org/10.1002/admi.201701370.
69. Vorobyev AY, Guo C. Direct femtosecond laser surface nano/microstructuring and its applications. Laser Photonics Rev. 2013;7:385–407. https://doi.org/10.1002/lpor.201200017.
70. Qiao M, Yan J, Jiang L. Direction Controllable Nano-Patterning of Titanium by Ultrafast Laser for Surface Coloring and Optical Encryption. Adv Opt Mater. 2022;10:2101673. https://doi.org/10.1002/adom.202101673.
71. Bonse J, Gräf S. Maxwell Meets Marangoni—A Review of Theories on Laser-Induced Periodic Surface Structures. Laser Photonics Rev. 2020;14:2000215. https://doi.org/10.1002/lpor.202000215.
72. Shimotsuma Y, Kazansky PG, Qiu J, Hirao K. Self-Organized Nanogratings in Glass Irradiated by Ultrashort Light Pulses. Phys Rev Lett. 2003;91:247405. https://doi.org/10.1103/PhysRevLett.91.247405.
73. Öktem B, et al. Nonlinear laser lithography for indefinitely large-area nanostructuring with femtosecond pulses. Nat Photonics. 2013;7:897–901. https://doi.org/10.1038/nphoton.2013.272.

74. Mastellone M, et al. Deep-Subwavelength 2D Periodic Surface Nanostructures on Diamond by Double-Pulse Femtosecond Laser Irradiation. Nano Lett. 2021;21:4477–83. https://doi.org/10.1021/acs.nanolett.1c01310.
75. Sun X-C, et al. Wafer-scale high aspect-ratio sapphire periodic nanostructures fabricated by self-modulated femtosecond laser hybrid technology. Opt Express. 2022;30:32244–55. https://doi.org/10.1364/OE.463575.
76. Huang M, Zhao F, Cheng Y, Xu N, Xu Z. Origin of Laser-Induced Near-Subwavelength Ripples: Interference between Surface Plasmons and Incident Laser. ACS Nano. 2009;3:4062–70. https://doi.org/10.1021/nn900654v.
77. Liao Y, et al. High-fidelity visualization of formation of volume nanogratings in porous glass by femtosecond laser irradiation. Optica. 2015;2:329–34. https://doi.org/10.1364/OPTICA.2.000329.
78. Zhang B, et al. Self-organized phase-transition lithography for all-inorganic photonic textures. Light. 2021;10:93. https://doi.org/10.1038/s41377-021-00534-5.
79. Rudenko A, et al. Spontaneous periodic ordering on the surface and in the bulk of dielectrics irradiated by ultrafast laser: a shared electromagnetic origin. Sci Rep. 2017;7:12306. https://doi.org/10.1038/s41598-017-12502-4.
80. Beresna M, Gecevičius M, Kazansky PG. Ultrafast laser direct writing and nanostructuring in transparent materials. Adv Opt Photon. 2014;6:293–339. https://doi.org/10.1364/AOP.6.000293.
81. Buividas R, et al. Mechanism of fine ripple formation on surfaces of (semi)transparent materials via a half-wavelength cavity feedback. Nanotechnology. 2011;22:055304. https://doi.org/10.1088/0957-4484/22/5/055304.
82. Beresna M, Gecevičius M, Lancry M, Poumellec B, Kazansky PG. Broadband anisotropy of femtosecond laser induced nanogratings in fused silica. Appl Phys Lett. 2013;103:131903. https://doi.org/10.1063/1.4821513.
83. Cho S-H, Kumagai H, Midorikawa K. In situ observation of dynamics of plasma formation and refractive index modification in silica glasses excited by a femtosecond laser. Optics Communications. 2002;207:243–53. https://doi.org/10.1016/S0030-4018(02)01410-4.
84. Davis KM, Miura K, Sugimoto N, Hirao K. Writing waveguides in glass with a femtosecond laser. Opt Lett. 1996;21:1729–31. https://doi.org/10.1364/OL.21.001729.
85. Buividas R, Mikutis M, Juodkazis S. Surface and bulk structuring of materials by ripples with long and short laser pulses: Recent advances. Prog Quantum Electron. 2014;38:119–56. https://doi.org/10.1016/j.pquantelec.2014.03.002.
86. Sudrie L, Franco M, Prade B, Mysyrowicz A. Writing of permanent birefringent microlayers in bulk fused silica with femtosecond laser pulses. Opt Commun. 1999;171:279–84. https://doi.org/10.1016/S0030-4018(99)00562-3.
87. Kazansky PG, et al. Anomalous Anisotropic Light Scattering in Ge-Doped Silica Glass. Phys Rev Lett. 1999;82:2199–202. https://doi.org/10.1103/PhysRevLett.82.2199.
88. Qiu J, et al. Memorized polarization-dependent light scattering in rare-earth-ion-doped glass. Appl Phys Lett. 2000;77:1940–2. https://doi.org/10.1063/1.1311956.
89. Hnatovsky C, et al. Pulse duration dependence of femtosecond-laser-fabricated nanogratings in fused silica. Appl Phys Lett. 2005;87:014104. https://doi.org/10.1063/1.1991991.
90. Taylor R, Hnatovsky C, Simova E. Applications of femtosecond laser induced self-organized planar nanocracks inside fused silica glass. Laser Photonics Rev. 2008;2:26–46. https://doi.org/10.1002/lpor.200710031.
91. Hnatovsky C, et al. Fabrication of microchannels in glass using focused femtosecond laser radiation and selective chemical etching. Appl Phys A. 2006;84:47–61. https://doi.org/10.1007/s00339-006-3590-4.
92. Sudrie L, et al. Femtosecond Laser-Induced Damage and Filamentary Propagation in Fused Silica. Phys Rev Lett. 2002;89:186601. https://doi.org/10.1103/PhysRevLett.89.186601.
93. Ohfuchi T, et al. Shape control of femtosecond-laser-induced birefringent structures by controlling spherical aberration. J Laser Appl. 2016;28:022603. https://doi.org/10.2351/1.4944115.
94. Lancry M, Brisset F, Poumellec B. In the heart of nanogratings made up during femtosecond laser irradiation, in Advanced Photonics & Renewable Energy, OSA Technical Digest (CD) (Optica Publishing Group, 2010), paper BWC3. https://opg.optica.org/abstract.cfm?URI=BGPP-2010-BWC3.
95. Ramirez LPR, et al. Tuning the structural properties of femtosecond-laser-induced nanogratings. Appl Phys A. 2010;100:1–6. https://doi.org/10.1007/s00339-010-5684-2.
96. Zhang F, Zhang H, Dong G, Qiu J. Embedded nanogratings in germanium dioxide glass induced by femtosecond laser direct writing. J Opt Soc Am B. 2014;31:860–4. https://doi.org/10.1364/JOSAB.31.000860.
97. Hnatovsky C, et al. Polarization-selective etching in femtosecond laser-assisted microfluidic channel fabrication in fused silica. Opt Lett. 2005;30:1867–9. https://doi.org/10.1364/OL.30.001867.
98. Taylor RS, et al. Femtosecond laser erasing and rewriting of self-organized planar nanocracks in fused silica glass. Opt Lett. 2007;32:2888–90. https://doi.org/10.1364/OL.32.002888.
99. Bricchi E, Kazansky PG. Extraordinary stability of anisotropic femtosecond direct-written structures embedded in silica glass. Appl Phys Lett. 2006;88:111119. https://doi.org/10.1063/1.2185587.
100. Richter S, et al. Nanogratings in fused silica: Formation, control, and applications. J Laser Appl. 2012;24:042008. https://doi.org/10.2351/1.4718561.
101. Wang J, Liu X, Dai Y, Wang Z, Qiu J. Effect of sodium oxide content on the formation of nanogratings in germanate glass by a femtosecond laser. Opt Express. 2018;26:12761–8. https://doi.org/10.1364/OE.26.012761.
102. Asai T, et al. Systematic Control of Structural Changes in GeO2 Glass Induced by Femtosecond Laser Direct Writing. J Am Ceram Soc. 2015;98:1471–7. https://doi.org/10.1111/jace.13482.
103. Lancry M, et al. Ultrafast nanoporous silica formation driven by femtosecond laser irradiation. Laser Photonics Rev. 2013;7:953–62. https://doi.org/10.1002/lpor.201300043.
104. Bricchi E, Klappauf BG, Kazansky PG. Form birefringence and negative index change created by femtosecond direct writing in transparent materials. Opt Lett. 2004;29:119–21. https://doi.org/10.1364/OL.29.000119.
105. Hnatovsky C, Shvedov V, Krolikowski W, Rode A. Revealing Local Field Structure of Focused Ultrashort Pulses. Physical Review Letters. 2011;106:123901. https://doi.org/10.1103/PhysRevLett.106.123901.
106. Shugaev MV, et al. Fundamentals of ultrafast laser–material interaction. MRS Bull. 2016;41:960–8. https://doi.org/10.1557/mrs.2016.274.
107. Musgraves JD, Richardson K, Jain H. Laser-induced structural modification, its mechanisms, and applications in glassy optical materials. Opt Mater Express. 2011;1:921–35. https://doi.org/10.1364/OME.1.000921.

108. Wang Y, Lancry M, Cavillon M, Poumellec B. Lifetime prediction of nanogratings inscribed by a femtosecond laser in silica glass. Opt Lett. 2022;47:1242–5. https://doi.org/10.1364/OL.449486.
109. Richter S, et al. Laser induced nanogratings beyond fused silica - periodic nanostructures in borosilicate glasses and ULE™. Opt Mater Express. 2013;3:1161–6. https://doi.org/10.1364/OME.3.001161.
110. Cao J, et al. Form birefringence induced in multicomponent glass by femtosecond laser direct writing. Opt Lett. 2016;41:2739–42. https://doi.org/10.1364/OL.41.002739.
111. Cao J, Mazerolles L, Lancry M, Brisset F, Poumellec B. Modifications in lithium niobium silicate glass by femtosecond laser direct writing: morphology, crystallization, and nanostructure. J Opt Soc Am B. 2017;34:160–8. https://doi.org/10.1364/JOSAB.34.000160.
112. Cao J, Poumellec B, Brisset F, Lancry M. Pulse energy dependence of refractive index change in lithium niobium silicate glass during femtosecond laser direct writing. Opt Express. 2018;26:7460–74. https://doi.org/10.1364/OE.26.007460.
113. Cao J, et al. Femtosecond Laser-Induced Crystallization in Glasses: Growth Dynamics for Orientable Nanostructure and Nanocrystallization. Cryst Growth Des. 2019;19:2189–205. https://doi.org/10.1021/acs.cgd.8b01802.
114. Shimotsuma Y, et al. Self-assembled glass/crystal periodic nanostructure in Al2O3-Dy2O3 binary glass. Appl Phys A. 2018;124:82. https://doi.org/10.1007/s00339-017-1507-z.
115. Zhang B, et al. Self-Organized Periodic Crystallization in Unconventional Glass Created by an Ultrafast Laser for Optical Attenuation in the Broadband Near-Infrared Region. Advanced Optical Materials. 2019;7:1900593. https://doi.org/10.1002/adom.201900593.
116. Zhang B, et al. Ultrafast Laser Inducing Continuous Periodic Crystallization in the Glass Activated via Laser-Prepared Crystallite-Seeds. Adv Opt Mater. 2021;9:2001962. https://doi.org/10.1002/adom.202001962.
117. Kanehira S, Si J, Qiu J, Fujita K, Hirao K. Periodic Nanovoid Structures via Femtosecond Laser Irradiation. Nano Lett. 2005;5:1591–5. https://doi.org/10.1021/nl0510154.
118. Song J, et al. Formation mechanism of self-organized voids in dielectrics induced by tightly focused femtosecond laser pulses. Appl Phys Lett. 2008;92:092904. https://doi.org/10.1063/1.2841066.
119. Song J, et al. Polarization dependence of the self-organized microgratings induced in SrTiO3 crystal by a single femtosecond laser beam. Opt Express. 2013;21:18461–8. https://doi.org/10.1364/OE.21.018461.
120. Hu X, et al. Self-formation of quasiperiodic void structure in CaF2 induced by femtosecond laser irradiation. Journal of Applied Physics. 2007;101:023112. https://doi.org/10.1063/1.2430911.
121. Hu X, et al. Self-formation of void array in Al2O3 crystal by femtosecond laser irradiation. Chin Opt Lett. 2008;6:388–90.
122. Mauclair C, et al. Single-pulse ultrafast laser imprinting of axial dot arrays in bulk glasses. Opt Lett. 2011;36:325–7. https://doi.org/10.1364/OL.36.000325.
123. Hu X, et al. Self-organized microvoid array perpendicular to the femtosecond laser beam in CaF2 crystals. Laser Phys Lett. 2008;5:394–7. https://doi.org/10.1002/lapl.200810006.
124. Song J, et al. Mechanism of femtosecond laser inducing inverted microstructures by employing different types of objective lens. J Phys D. 2011;44:495402. https://doi.org/10.1088/0022-3727/44/49/495402.
125. Luo F, et al. Femtosecond laser-induced inverted microstructures inside glasses by tuning refractive index of objective's immersion liquid. Opt Lett. 2011;36:2125–7. https://doi.org/10.1364/OL.36.002125.
126. Zhang F, et al. Polarization-dependent microstructural evolution induced by a femtosecond laser in an aluminosilicate glass. Opt Express. 2021;29:10265–74. https://doi.org/10.1364/OE.420595.
127. Sakakura M, Lei Y, Wang L, Yu Y-H, Kazansky PG. Ultralow-loss geometric phase and polarization shaping by ultrafast laser writing in silica glass. Light. 2020;9:15. https://doi.org/10.1038/s41377-020-0250-y.
128. Zhang F, et al. Self-assembled three-dimensional periodic micro-nano structures in bulk quartz crystal induced by femtosecond laser pulses. Opt Express. 2019;27:6442–50. https://doi.org/10.1364/OE.27.006442.
129. Zhang F, et al. Evolution of polarization dependent microstructures induced by high repetition rate femtosecond laser irradiation in glass. Opt Express. 2016;24:21353–63. https://doi.org/10.1364/OE.24.021353.
130. Karpinski P, Shvedov V, Krolikowski W, Hnatovsky C. Laser-writing inside uniaxially birefringent crystals: fine morphology of ultrashort pulse-induced changes in lithium niobate. Opt Express. 2016;24:7456–76. https://doi.org/10.1364/OE.24.007456.
131. Xu S, et al. Ultrafast laser-inscribed nanogratings in sapphire for geometric phase elements. Opt Lett. 2021;46:536–9. https://doi.org/10.1364/OL.413177.
132. Zhai Q, et al. Evolution of self-organized nanograting from the pre-induced nanocrack-assisted plasma–laser coupling in sapphire. Appl Phys B. 2021;127:74. https://doi.org/10.1007/s00340-021-07625-6.
133. Liu Z, et al. Three-Dimensional Self-Organization in Nanocomposite Layered Systems by Ultrafast Laser Pulses. ACS Nano. 2017;11:5031–40. https://doi.org/10.1021/acsnano.7b01748.
134. Loeschner K, Seifert G, Heilmann A. Self-organized, gratinglike nanostructures in polymer films with embedded metal nanoparticles induced by femtosecond laser irradiation. J Appl Phys. 2010;108:073114. https://doi.org/10.1063/1.3490191.
135. Eles B, et al. Mechanisms driving self-organization phenomena in random plasmonic metasurfaces under multipulse femtosecond laser exposure: a multitime scale study. 2022;11, 2303-2318, https://doi.org/10.1515/nanoph-2022-0023
136. Wu, B. et al. (2023). Plasmon guided assembly of nanoparticles in solids. Materials Today Nano 21, 100299, https://doi.org/10.1016/j.mtnano.2022.100299.
137. Shimotsuma Y, Hirao K, Qiu J, Kazansky PG. Nano-modification inside transparent materials by femtosecond laser single beam. Mod Phys Lett B. 2005;19:225–38. https://doi.org/10.1142/S0217984905008281.
138. Rudenko A, Colombier J-P, Itina TE. From random inhomogeneities to periodic nanostructures induced in bulk silica by ultrashort laser. Physical Review B. 2016;93:075427. https://doi.org/10.1103/PhysRevB.93.075427.
139. Rudenko A, Colombier J-P, Itina TE, Stoian R. Genesis of Nanogratings in Silica Bulk via Multipulse Interplay of Ultrafast Photo-Excitation and Hydrodynamics. Adv Opt Mater. 2021;9:2100973. https://doi.org/10.1002/adom.202100973.

140. Muzi E, Cavillon M, Lancry M, Brisset F, Que R, Pugliese D, et al. Towards a Rationalization of Ultrafast Laser-Induced Crystallization in Lithium Niobium Borosilicate Glasses: The Key Role of the Scanning Speed. Crystals. 2021;11(3):290. https://doi.org/10.3390/cryst11030290.
141. Bhardwaj VR, et al. Optically Produced Arrays of Planar Nanostructures inside Fused Silica. Phys Rev Lett. 2006;96:057404. https://doi.org/10.1103/PhysRevLett.96.057404.
142. Rajeev PP, et al. Transient nanoplasmonics inside dielectrics. J Phys B: At Mol Opt Phys. 2007;40:S273–82. https://doi.org/10.1088/0953-4075/40/11/s03.
143. Sun H, et al. Standing electron plasma wave mechanism of void array formation inside glass by femtosecond laser irradiation. Appl Phys A. 2007;88:285–8. https://doi.org/10.1007/s00339-007-4012-y.
144. Liao Y, et al. Formation of in-volume nanogratings with sub-100-nm periods in glass by femtosecond laser irradiation. Opt Lett. 2015;40:3623–6. https://doi.org/10.1364/OL.40.003623.
145. Lei Y, et al. High speed ultrafast laser anisotropic nanostructuring by energy deposition control via near-field enhancement. Optica. 2021;8:1365–71. https://doi.org/10.1364/OPTICA.433765.
146. Yan Z, Gao J, Beresna M, Zhang J. Near-Field Mediated 40 nm In-Volume Glass Fabrication by Femtosecond Laser. Adv Opt Mater. 2022;10:2101676. https://doi.org/10.1002/adom.202101676.
147. Martin P, et al. Subpicosecond study of carrier trapping dynamics in wide-band-gap crystals. Phys Rev B. 1997;55:5799–810. https://doi.org/10.1103/PhysRevB.55.5799.
148. Petite G, Daguzan P, Guizard S, Martin P. Conduction electrons in wide-bandgap oxides: a subpicosecond time-resolved optical study. Nucl Instrum Methods Phys Res, Sect B. 1996;107:97–101. https://doi.org/10.1016/0168-583X(95)00845-4.
149. Richter S, et al. The role of self-trapped excitons and defects in the formation of nanogratings in fused silica. Opt Lett. 2012;37:482–4. https://doi.org/10.1364/OL.37.000482.
150. Dai Y, Wu G, Lin X, Ma G, Qiu J. Femtosecond laser induced rotated 3D self-organized nanograting in fused silica. Opt Express. 2012;20:18072–8. https://doi.org/10.1364/OE.20.018072.
151. Lei Y, et al. Efficient ultrafast laser writing with elliptical polarization. Light. 2023;12:74. https://doi.org/10.1038/s41377-023-01098-2.
152. Gaizauskas E, et al. Discrete damage traces from filamentation of Gauss-Bessel pulses. Opt Lett. 2006;31:80–2. https://doi.org/10.1364/OL.31.000080.
153. Bricchi E, Mills JD, Kazansky PG, Klappauf BG, Baumberg JJ. Birefringent Fresnel zone plates in silica fabricated by femtosecond laser machining. Opt Lett. 2002;27:2200–2. https://doi.org/10.1364/OL.27.002200.
154. Tian J, et al. A Comparison between Nanogratings-Based and Stress-Engineered Waveplates Written by Femtosecond Laser in Silica. Micromachines. 2020;11, https://doi.org/10.3390/mi11020131
155. Ohfuchi T, et al. Polarization imaging camera with a waveplate array fabricated with a femtosecond laser inside silica glass. Opt Express. 2017;25:23738–54. https://doi.org/10.1364/OE.25.023738.
156. Lammers K, et al. Embedded nanograting-based waveplates for polarization control in integrated photonic circuits. Opt Mater Express. 2019;9:2560–72. https://doi.org/10.1364/OME.9.002560.
157. Beresna M, Kazansky PG. Polarization diffraction grating produced by femtosecond laser nanostructuring in glass. Opt Lett. 2010;35:1662–4. https://doi.org/10.1364/OL.35.001662.
158. Cai W, Libertun AR, Piestun R. Polarization selective computer-generated holograms realized in glass by femtosecond laser induced nanogratings. Opt Express. 2006;14:3785–91. https://doi.org/10.1364/OE.14.003785.
159. Zhang F, Yu Y, Cheng C, Dai Y, Qiu J. Fabrication of polarization-dependent light attenuator in fused silica using a low-repetition-rate femtosecond laser. Opt Lett. 2013;38:2212–4. https://doi.org/10.1364/OL.38.002212.
160. Zhang F, et al. Wavelength response and thermal stability of embedded nanograting structure light attenuator fabricated by direct femtosecond laser writing. Appl Phys B. 2014;117:53–8. https://doi.org/10.1007/s00340-014-5797-y.
161. Cavillon M, et al. Overview of high temperature fibre Bragg gratings and potential improvement using highly doped aluminosilicate glass optical fibres. J Phys. 2019;1:042001. https://doi.org/10.1088/2515-7647/ab382f.
162. Mihailov SJ, Hnatovsky C, Grobnic D, Chen K, Li M. Fabrication of Bragg Gratings in Random Air-Line Clad Microstructured Optical Fiber. IEEE Photonics Technol Lett. 2018;30:209–12. https://doi.org/10.1109/LPT.2017.2782368.
163. Hnatovsky C, Grobnic D, Coulas D, Barnes M, Mihailov SJ. Self-organized nanostructure formation during femtosecond-laser inscription of fiber Bragg gratings. Opt Lett. 2017;42:399–402. https://doi.org/10.1364/OL.42.000399.
164. Li J, Ho S, Haque M, Herman PR. Nanograting Bragg responses of femtosecond laser written optical waveguides in fused silica glass. Opt Mater Express. 2012;2:1562–70. https://doi.org/10.1364/OME.2.001562.
165. Beresna M, Gecevičius M, Kazansky PG, Gertus T. Radially polarized optical vortex converter created by femtosecond laser nanostructuring of glass. Appl Phys Lett. 2011;98:201101. https://doi.org/10.1063/1.3590716.
166. Zhang F, Cerkauskaite A, Drevinskas R, Kazansky PG, Qiu J. Microengineering of Optical Properties of GeO2 Glass by Ultrafast Laser Nanostructuring. Adv Opt Mater. 2017;5:1700342. https://doi.org/10.1002/adom.201700342.
167. Beresna M, Gecevičius M, Kazansky PG. Polarization sensitive elements fabricated by femtosecond laser nanostructuring of glass [Invited]. Opt Mater Express. 2011;1:783–95. https://doi.org/10.1364/OME.1.000783.
168. Zhang B, Liu X, Qiu J. Single femtosecond laser beam induced nanogratings in transparent media - Mechanisms and applications. J Materiomics. 2019;5:1–14. https://doi.org/10.1016/j.jmat.2019.01.002.
169. Lu J, et al. Fiber nanogratings induced by femtosecond pulse laser direct writing for in-line polarizer. Nanoscale. 2019;11:908–14. https://doi.org/10.1039/C8NR06078A.
170. He J, Xu B, Xu X, Liao C, Wang Y. Review of Femtosecond-Laser-Inscribed Fiber Bragg Gratings: Fabrication Technologies and Sensing Applications. Photonic Sens. 2021;11:203–26. https://doi.org/10.1007/s13320-021-0629-2.
171. Pallarés-Aldeiturriaga, D., Roldán-Varona, P., Rodríguez-Cobo, L. López-Higuera, J. M. (2020).Optical Fiber Sensors by Direct Laser Processing: A Review. Sensors 20, https://doi.org/10.3390/s20236971
172. Wang M, et al. Femtosecond laser fabrication of nanograting-based distributed fiber sensors for extreme environmental applications. Int J Extreme Manuf. 2021;3:025401. https://doi.org/10.1088/2631-7990/abe171.
173. Kaisler S, Armour F, Espinosa JA. Money, W. in 2013 46th Hawaii International Conference on System Sciences. 995–1004.
174. Gu M, Zhang Q, Lamon S. Nanomaterials for optical data storage. Nat Rev Mater. 2016;1:16070. https://doi.org/10.1038/natrevmats.2016.70.

175. Zhang Q, Xia Z, Cheng Y-B, Gu M. High-capacity optical long data memory based on enhanced Young's modulus in nanoplasmonic hybrid glass composites. Nat Commun. 2018;9:1183. https://doi.org/10.1038/s41467-018-03589-y.
176. Gu M, Li X, Cao Y. Optical storage arrays: a perspective for future big data storage. Light. 2014;3:e177–e177. https://doi.org/10.1038/lsa.2014.58.
177. Zhu L, et al. Near-perfect fidelity polarization-encoded multilayer optical data storage based on aligned gold nanorods. Opto-Electronic Advances. 2021;4:210002. https://doi.org/10.29026/oea.2021.210002.
178. Wang Z, Zhang B, Tan D, Qiu J. Ostensibly perpetual optical data storage in glass with ultra-high stability and tailored photoluminescence. Opto-Electronic Advances. 2023;6, 220008–220001–220008–220008, https://doi.org/10.29026/oea.2023.220008
179. Shimotsuma Y, et al. Ultrafast Manipulation of Self-Assembled Form Birefringence in Glass. Adv Mater. 2010;22:4039–43. https://doi.org/10.1002/adma.201000921.
180. Zhang J, Gecevičius M, Beresna M, Kazansky PG. Seemingly Unlimited Lifetime Data Storage in Nanostructured Glass. Phys Rev Lett. 2014;112:033901. https://doi.org/10.1103/PhysRevLett.112.033901.
181. Yan Z, et al. Anisotropic nanostructure generated by a spatial-temporal manipulated picosecond pulse for multidimensional optical data storage. Opt Lett. 2021;46:5485–8. https://doi.org/10.1364/OL.443370.
182. Wang H, et al. 100-Layer Error-Free 5D Optical Data Storage by Ultrafast Laser Nanostructuring in Glass. Laser & Photonics Reviews 2022;n/a, 2100563, https://doi.org/10.1002/lpor.202100563
183. Liao Y, et al. Femtosecond laser nanostructuring in porous glass with sub-50 nm feature sizes. Opt Lett. 2013;38:187–9. https://doi.org/10.1364/OL.38.000187.
184. Liao Y, et al. Direct laser writing of sub-50 nm nanofluidic channels buried in glass for three-dimensional micro-nanofluidic integration. Lab Chip. 2013;13:1626–31. https://doi.org/10.1039/C3LC41171K.
185. Haque M, Lee KKC, Ho S, Fernandes LA, Herman PR. Chemical-assisted femtosecond laser writing of lab-in-fibers. Lab Chip. 2014;14:3817–29. https://doi.org/10.1039/C4LC00648H.
186. Ródenas A, et al. Three-dimensional femtosecond laser nanolithography of crystals. Nat Photonics. 2019;13:105–9. https://doi.org/10.1038/s41566-018-0327-9.
187. Sima F, et al. Three-dimensional femtosecond laser processing for lab-on-a-chip applications. 7, 613-634, doi:https://doi.org/10.1515/nanoph-2017-0097 (2018).
188. Osellame R, Hoekstra HJWM, Cerullo G, Pollnau M. Femtosecond laser microstructuring: an enabling tool for optofluidic lab-on-chips. Laser Photonics Rev. 2011;5:442–63. https://doi.org/10.1002/lpor.201000031.
189. Marcinkevičius A, et al. Femtosecond laser-assisted three-dimensional microfabrication in silica. Opt Lett. 2001;26:277–9. https://doi.org/10.1364/OL.26.000277.
190. Qi J, et al. Femtosecond laser induced selective etching in fused silica: optimization of the inscription conditions with a high-repetition-rate laser source. Opt Express. 2018;26:29669–78. https://doi.org/10.1364/OE.26.029669.
191. Yu X, et al. Tuning etch selectivity of fused silica irradiated by femtosecond laser pulses by controlling polarization of the writing pulses. J Appl Phys. 2011;109:053114. https://doi.org/10.1063/1.3555080.
192. Lu J, et al. Tailoring chiral optical properties by femtosecond laser direct writing in silica. Light. 2023;12:46. https://doi.org/10.1038/s41377-023-01080-y.
193. Ashoka A, et al. Extracting quantitative dielectric properties from pump-probe spectroscopy. Nat Commun. 2022;13:1437. https://doi.org/10.1038/s41467-022-29112-y.
194. Yao Y, et al. Single-Shot Real-Time Ultrafast Imaging of Femtosecond Laser Fabrication. ACS Photonics. 2021;8:738–44. https://doi.org/10.1021/acsphotonics.1c00043.
195. Yang C, et al. Single-Shot Receive-Only Ultrafast Electro-Optical Deflection Imaging. Phys Rev Appl. 2020;13:024001. https://doi.org/10.1103/PhysRevApplied.13.024001.
196. Lamon S, Wu Y, Zhang Q, Liu X, Gu M. Nanoscale optical writing through upconversion resonance energy transfer. Science Advances 7, eabe2209, https://doi.org/10.1126/sciadv.abe2209.
197. Salter PS, Booth MJ. Adaptive optics in laser processing. Light. 2019;8:110. https://doi.org/10.1038/s41377-019-0215-1.
198. Wang H, et al. Two-Photon Polymerization Lithography for Optics and Photonics: Fundamentals, Materials, Technologies, and Applications. Advanced Functional Materials. 2023; n/a, 2214211, https://doi.org/10.1002/adfm.202214211
199. Malevich P, et al. High energy and average power femtosecond laser for driving mid-infrared optical parametric amplifiers. Opt Lett. 2013;38:2746–9. https://doi.org/10.1364/OL.38.002746.
200. Fang X, Ren H, Gu M. Orbital angular momentum holography for high-security encryption. Nat Photonics. 2020;14:102–8. https://doi.org/10.1038/s41566-019-0560-x.
201. Xinyuan F, et al. High-dimensional orbital angular momentum multiplexing nonlinear holography. Adv Photonics. 2021;3:1–7. https://doi.org/10.1117/1.AP.3.1.015001.
202. Bozinovic N, et al. Terabit-Scale Orbital Angular Momentum Mode Division Multiplexing in Fibers. Science. 2013;340:1545–8. https://doi.org/10.1126/science.1237861.


## Publisher's Note

Springer Nature remains neutral with regard to jurisdictional claims in published maps and institutional affiliations.